

Outline

- Motivation and Background
- Materials Issues in Photoelectrocatalysis.
- High Throughput Photocatalyst Synthesis and Screening
- Observed Compositional And Morphological Dependencies in Metal Oxide Photocatalysts.

Motivation: It's Important

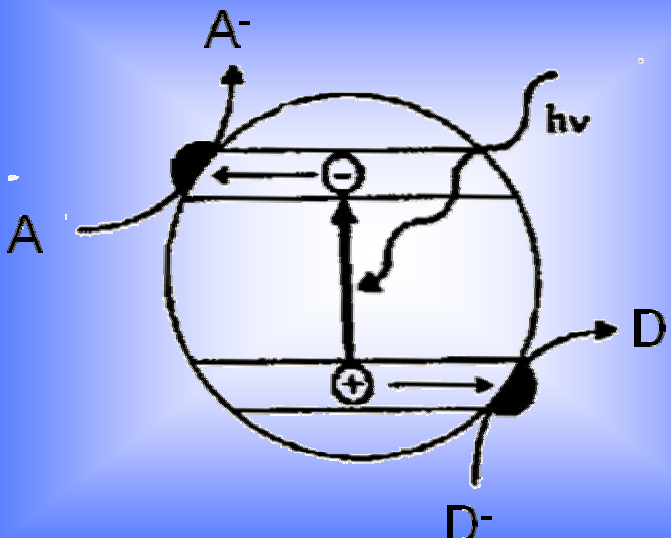


Motivation: It's Imaginable

Solar Energy Potential
US energy consumption $\sim 3 \times 10^{12}$ Watts
 $200 \text{ W/m}^2 @ 10\% \text{ efficiency} \rightarrow 390 \text{ km} \times 390 \text{ km area}$

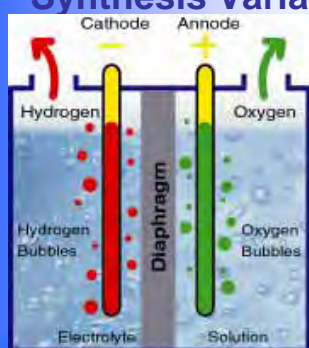


Motivation: It's Interesting



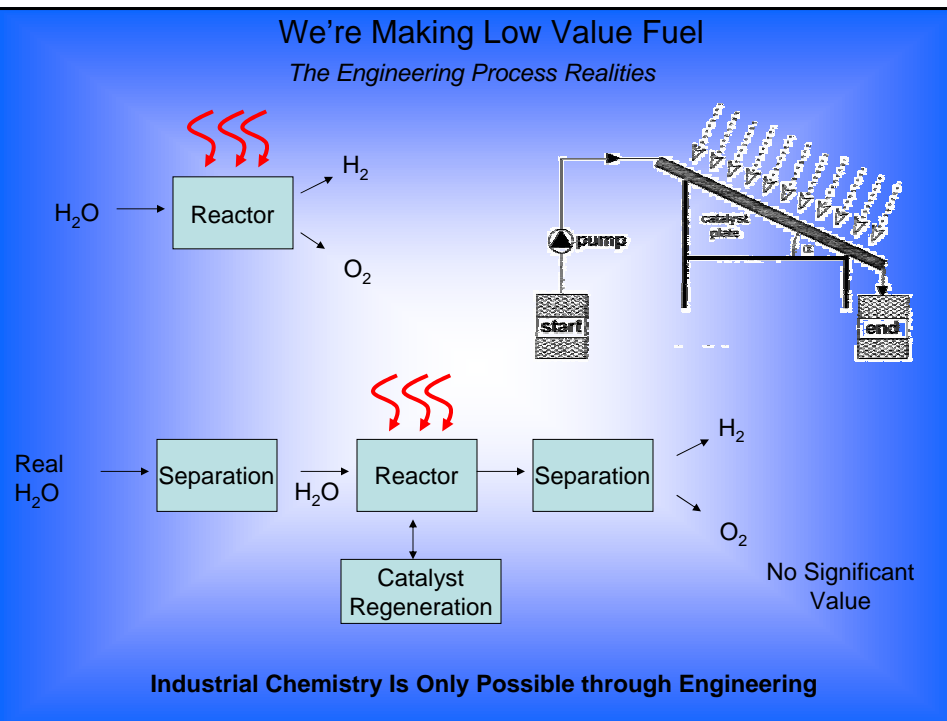
It's Just Solar Powered Electrosynthesis of Chemicals

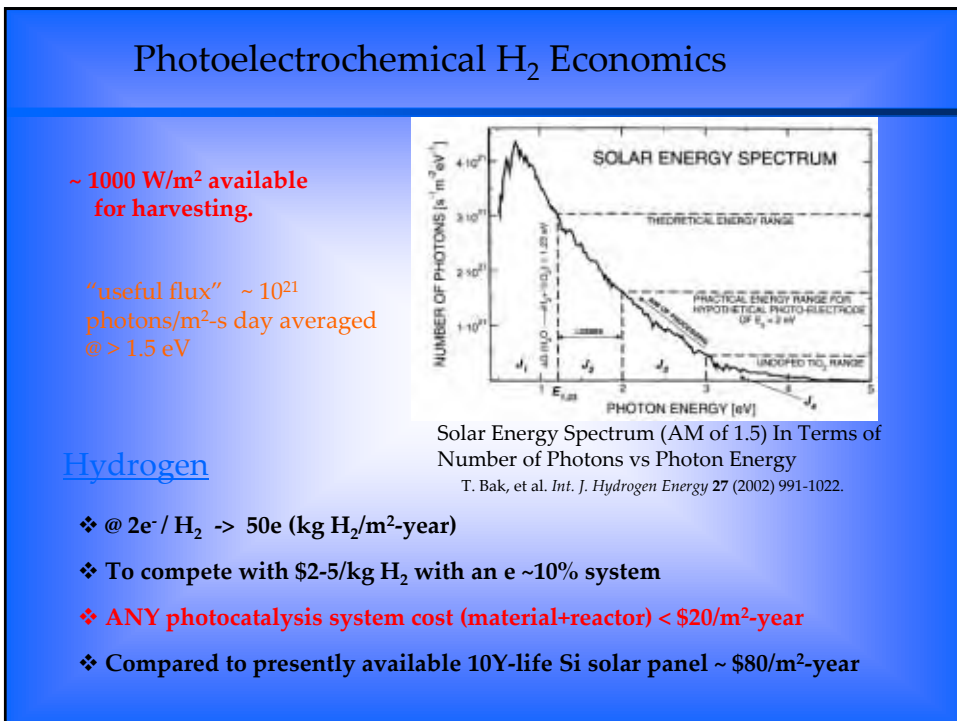
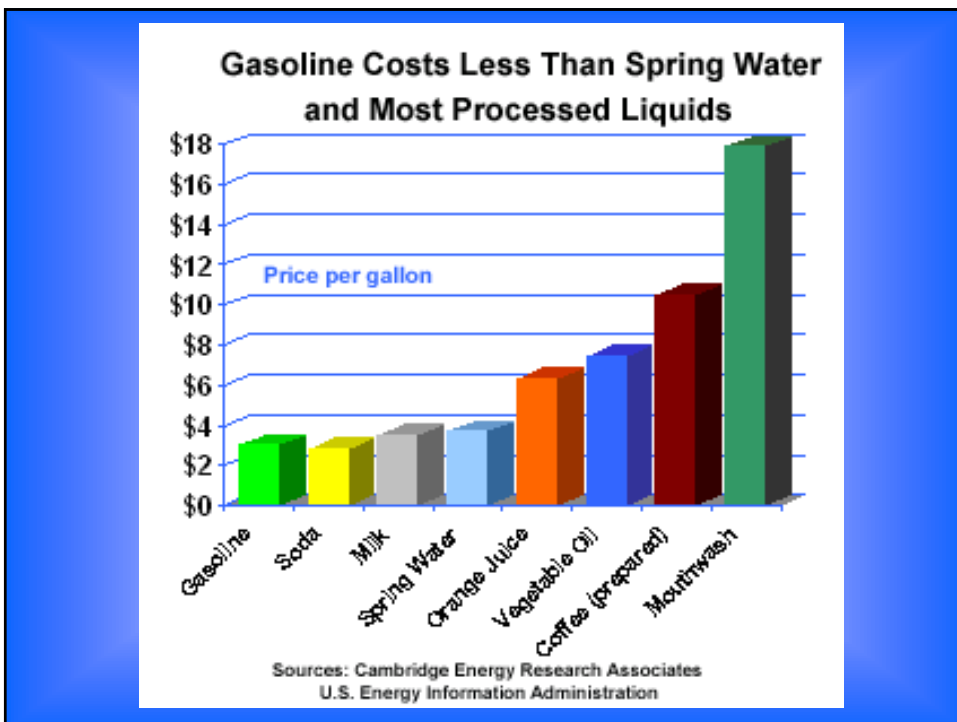
- Low Temperature
- Selective
- Wide Range of Synthesis Variables
- Art and “Magic”
- Relatively slow
- Electricity Cost
- Electrode Stability



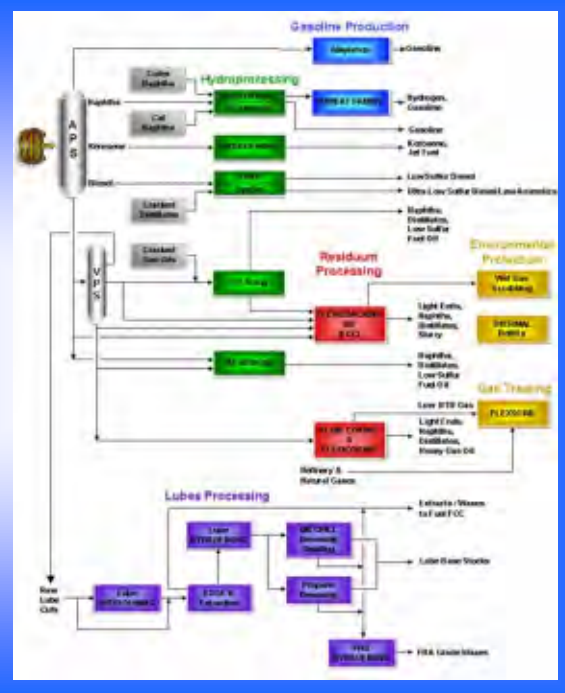
Photoelectrochemical Synthesis

- Low Temperature
- Selective
- Same Chemistries as Electrosynthesis
- Art and “Magic”
- Relatively slow
- Photon Costs
- Photon-Electron Conversion
- Material Stability

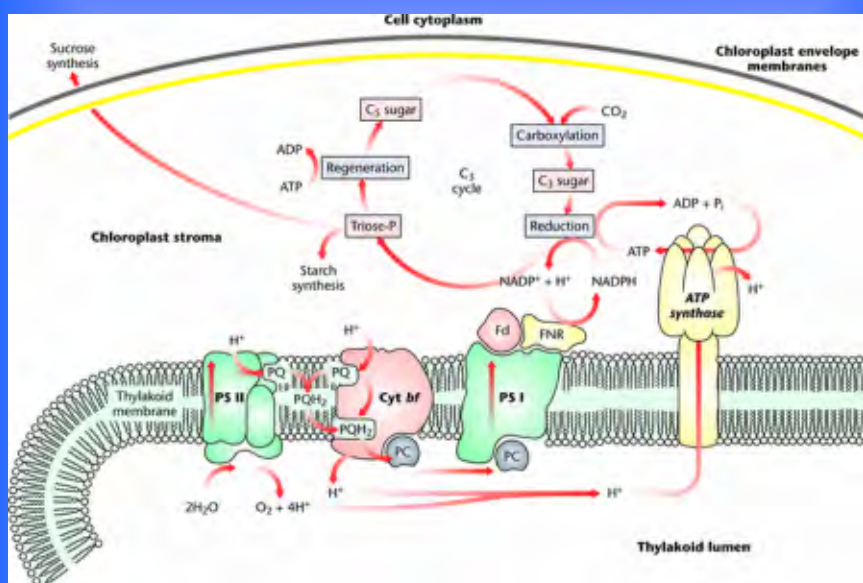


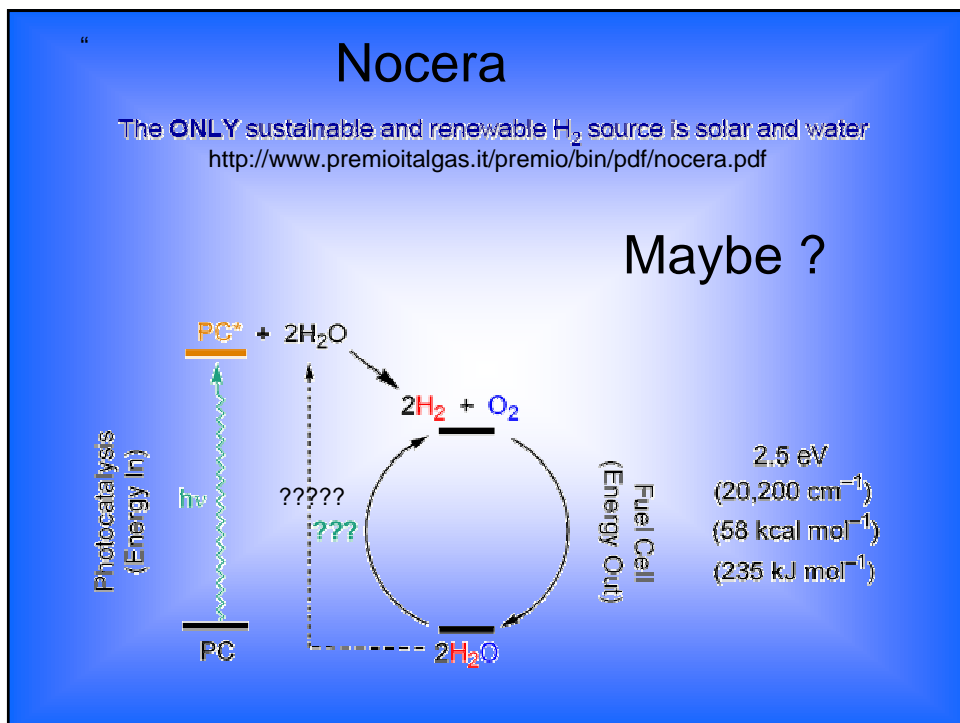
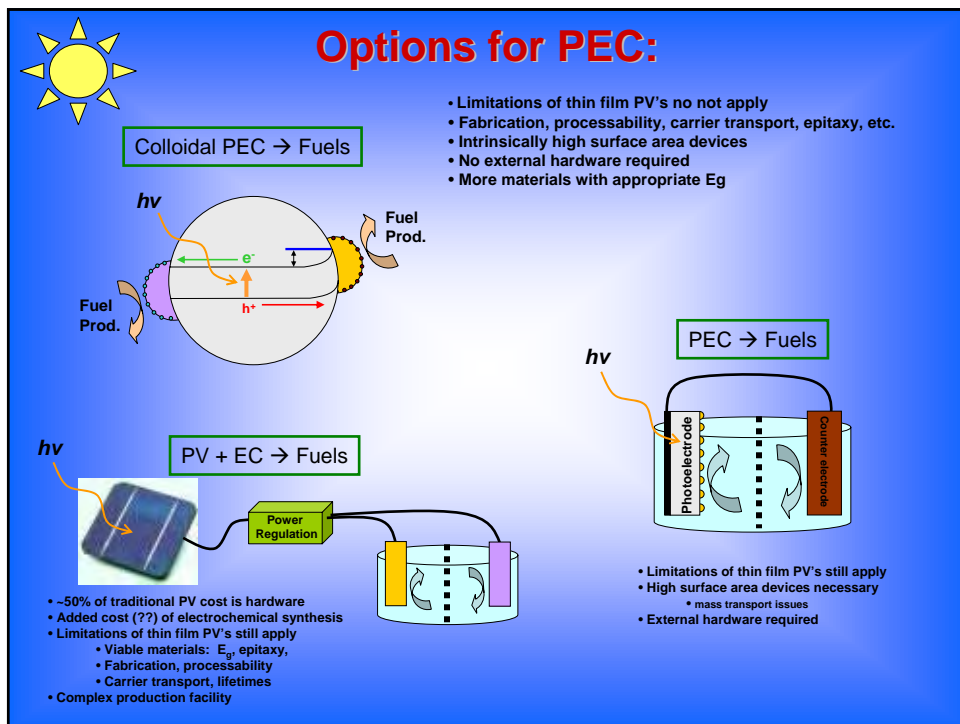


Oil → Gasoline is cheap because it is simple and can be integrated

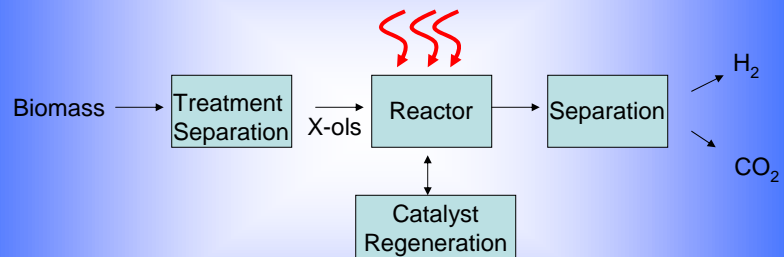


Process Integration

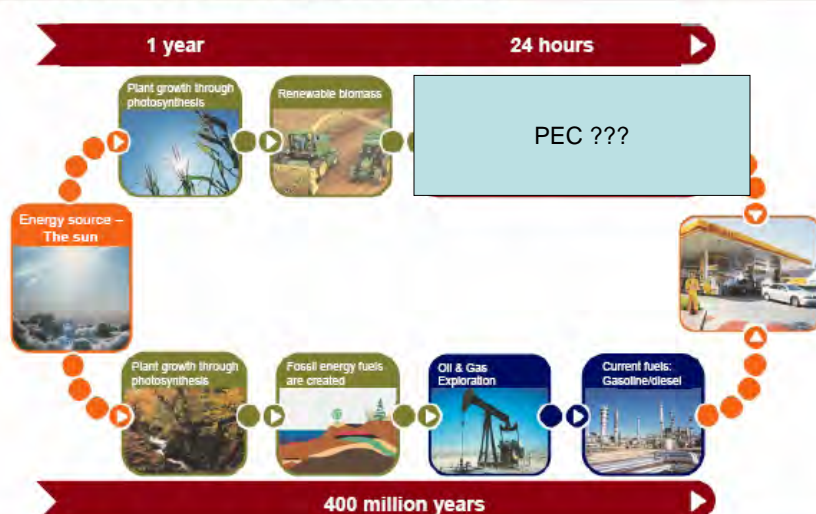


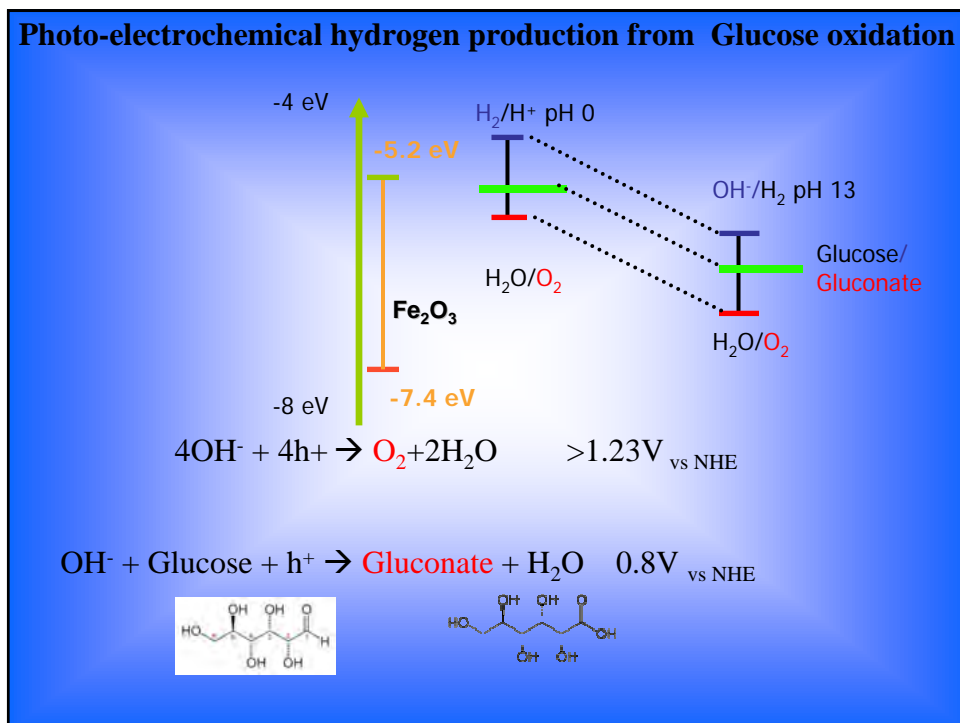
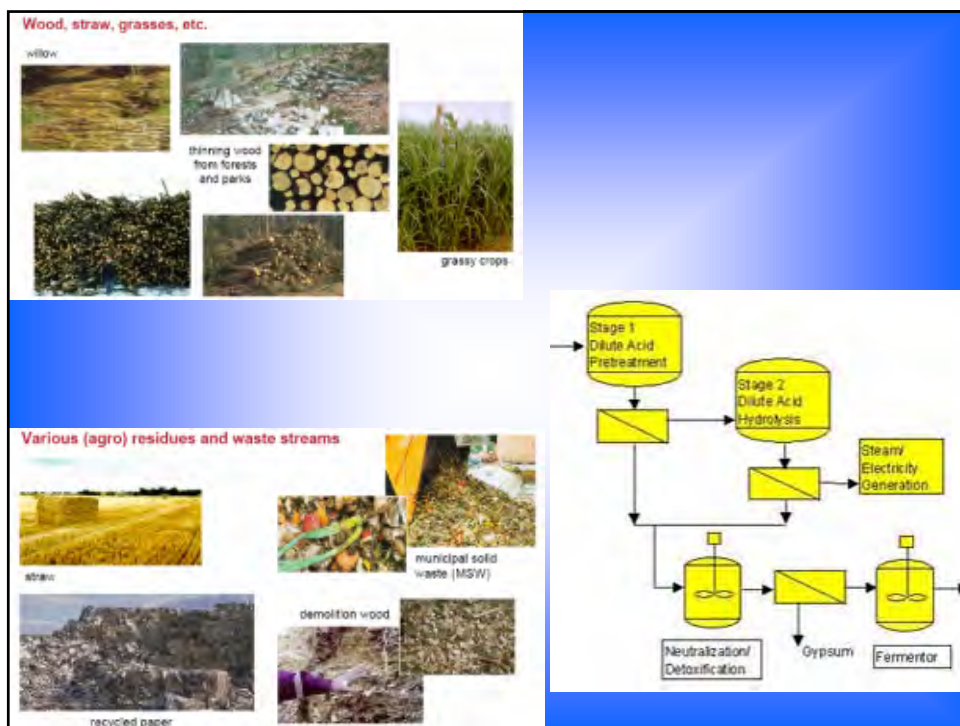


Process Alternatives: $C_nH_mO_z \rightarrow H_2 + CO_2$



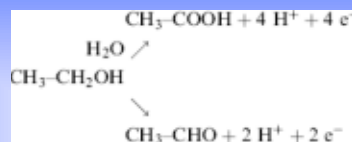
Following Nature's example – but much faster!



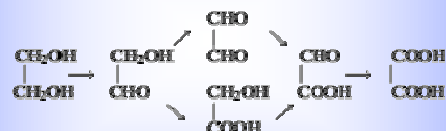


Electro-oxidation of Hydrocarbons

- $\text{CH}_3\text{CH}_2\text{OH}$

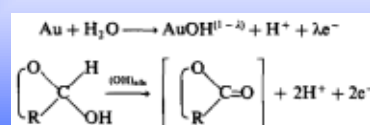


- $\text{HOCH}_2\text{CH}_2\text{OH}$



- Glucose

Journal of Applied Electrochemistry, 31, 799, 2001



Electrochimica Acta, 37, 357, 1992

Photoelectrolysis of HBr and HHI Using a Monolithic Combined Photoelectrochemical/Photovoltaic Device

Oscar Khaleel* and John A. Turner*^a

National Renewable Energy Laboratory, Golden, Colorado 80401, USA

The photoelectrolysis of HBr and HHI using a p -Gd₂O₃/P₂O₅/Ga₂O₃ photoelectrochemical/photovoltaic device is demonstrated. This device is a photovoltaic cell, voltage-biased with an integrated photoactive device. The device splits these acids directly via illumination, using light at the only energy input. Additionally, for these compounds, the device can simultaneously produce electrical energy. The HBr and HHI decomposition efficiency for this system, based on the short circuit current and the chemical potential of each compound, is 8.1 and 2.6%, respectively. The total conversion efficiency, including the harvested electrical energy, is 11.2 and 9.6%, respectively.

* 1998 The Electrochemical Society. 0169-0002/98/03-0112-8. © 1998, all rights reserved.

Manuscript submitted February 2, 1998; revised manuscript accepted March 30, 1998. Available electronically May 1, 1998.

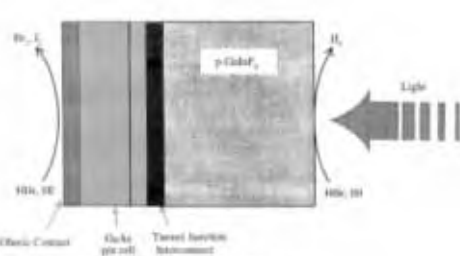
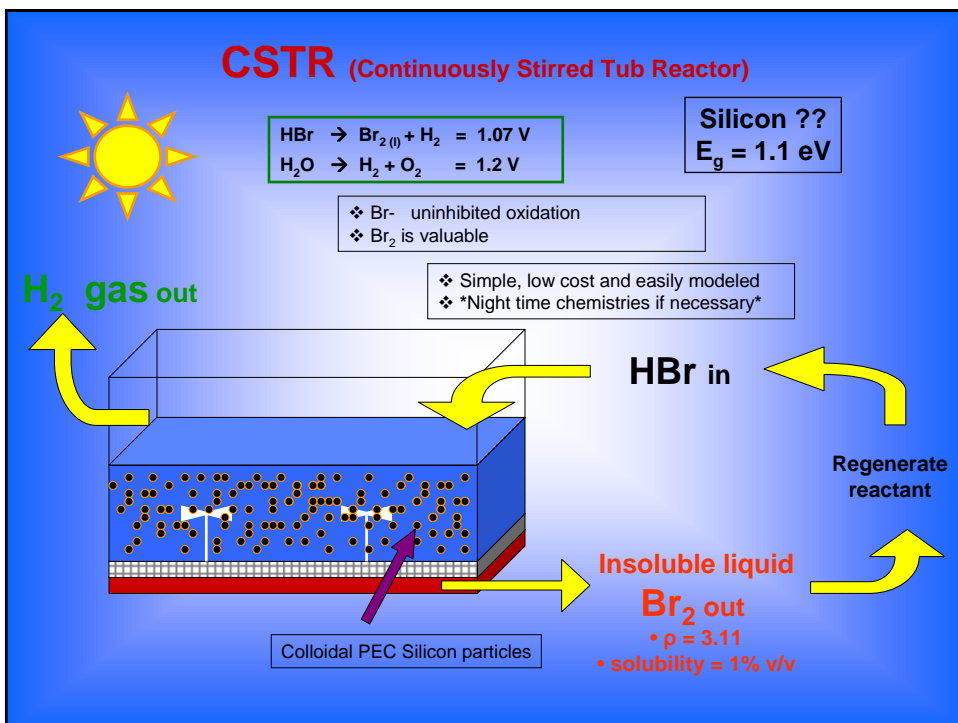
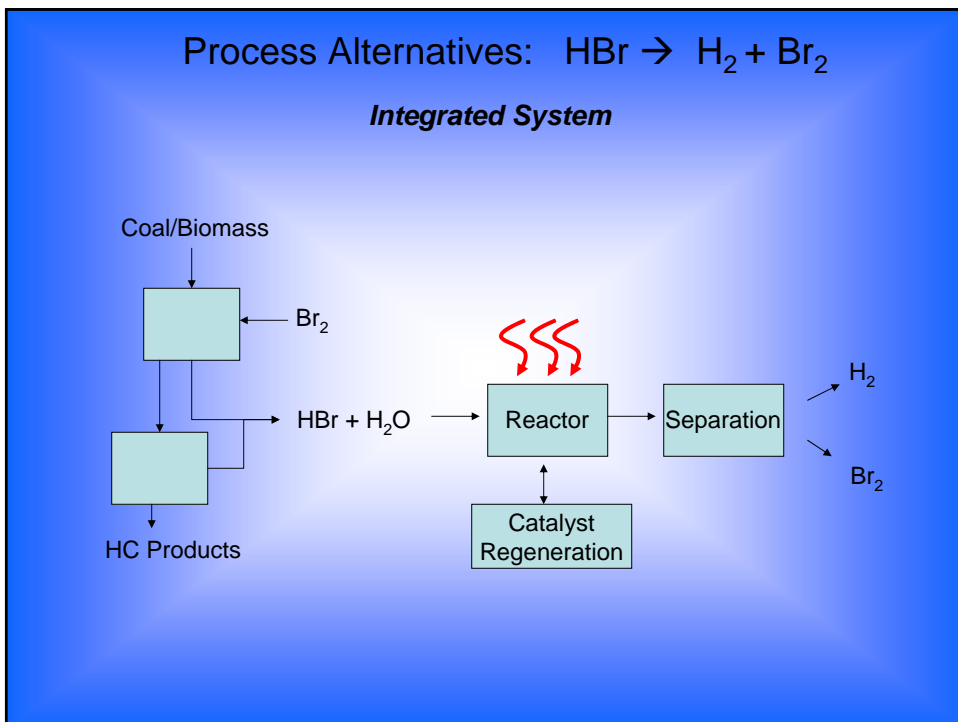


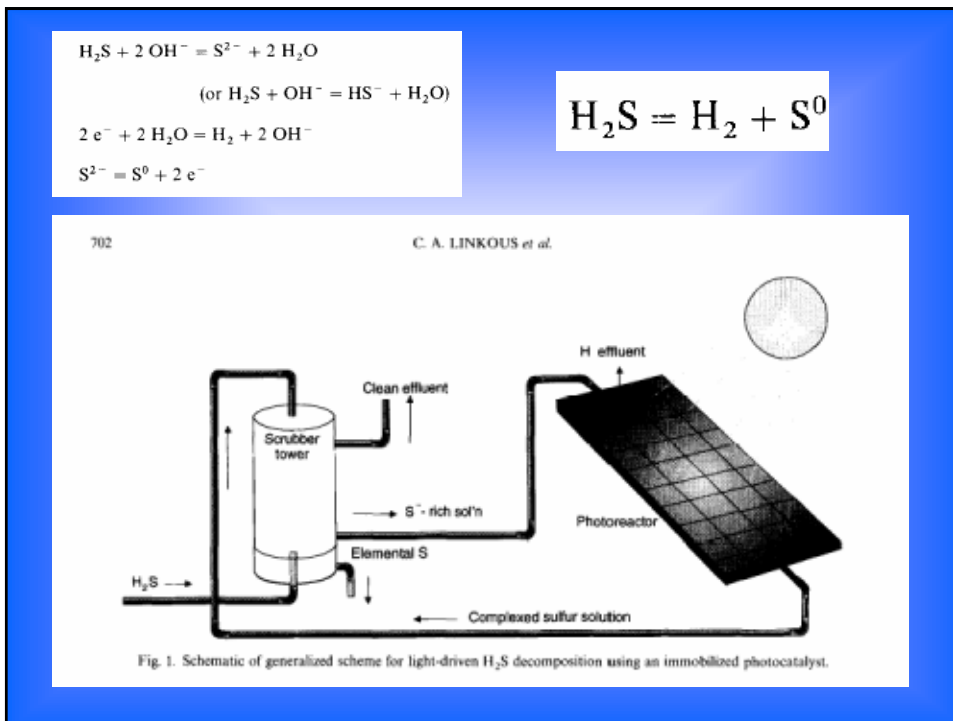
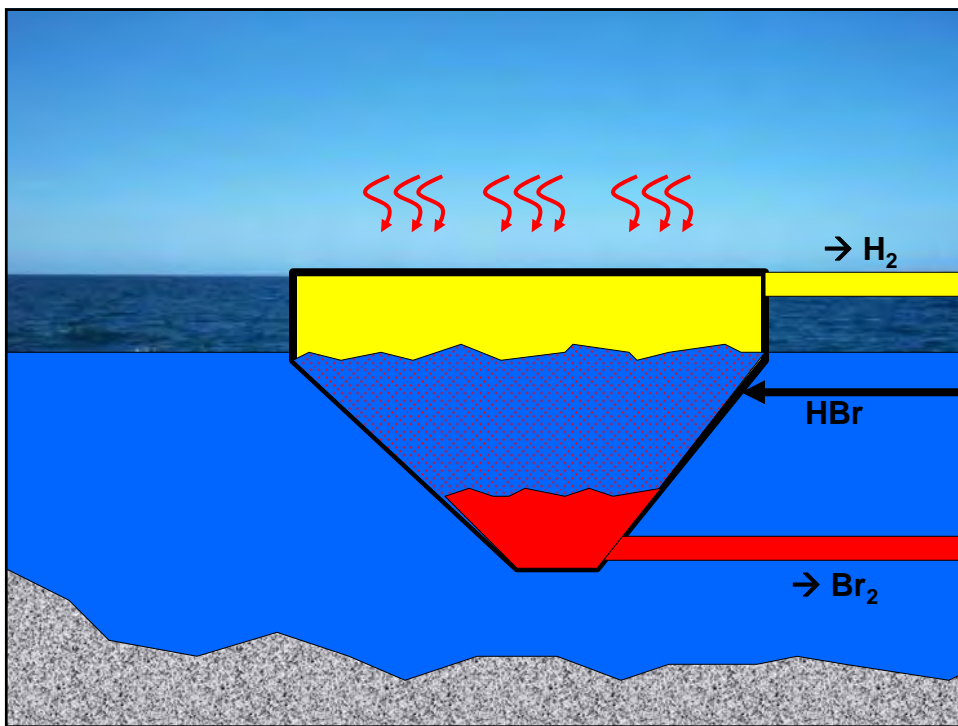
Figure 1. Schematic of a monolithic PEC/PV device.

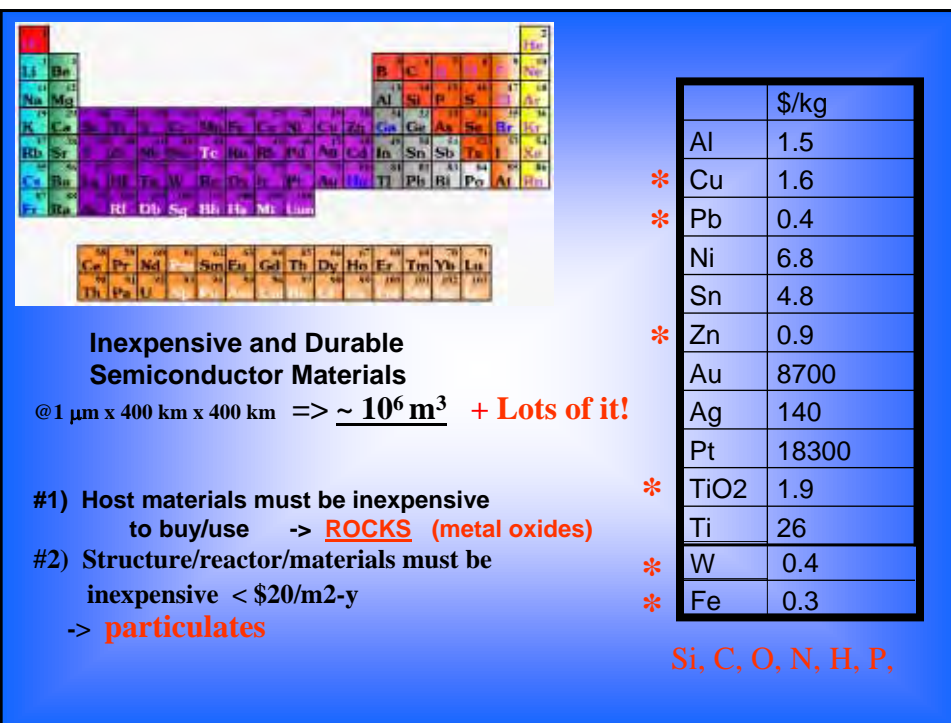
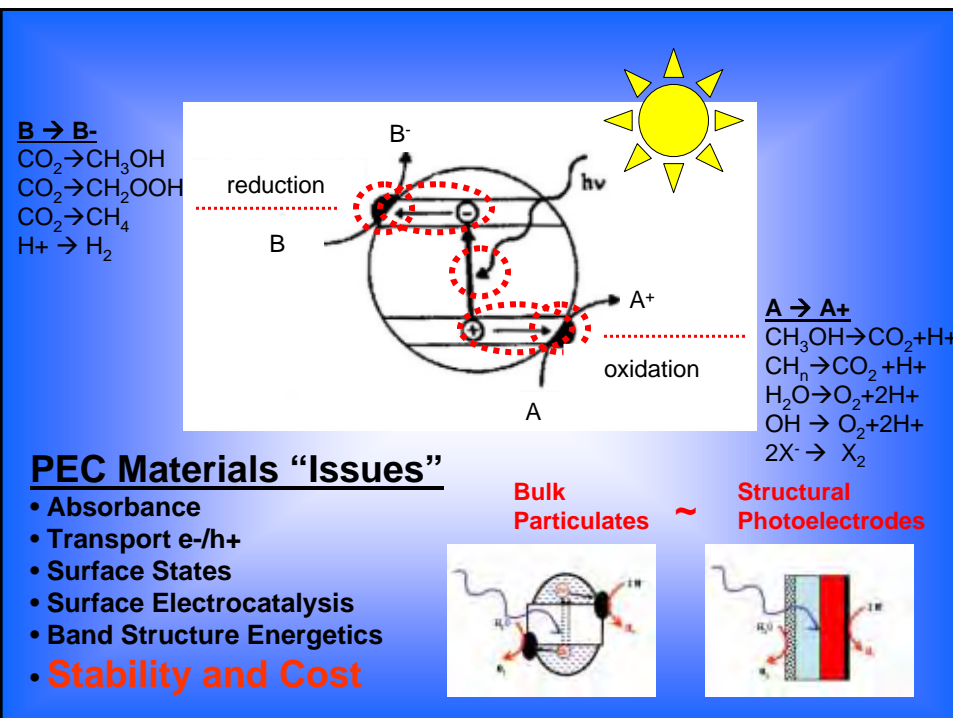
\$15/bbl oil

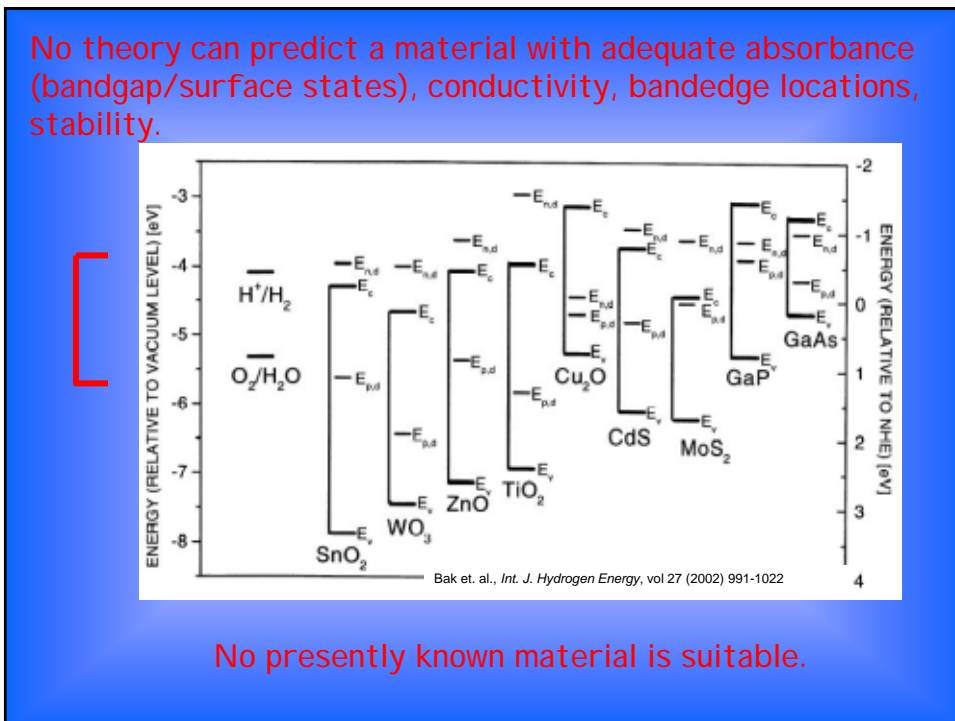
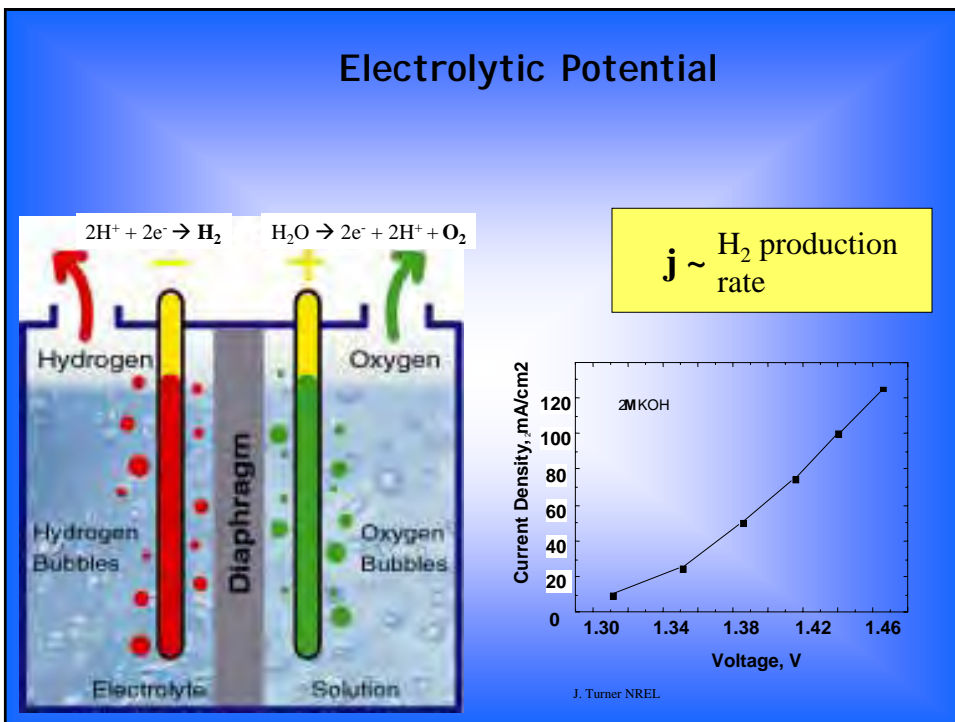
The splitting of HI and HBr is another possibility for solar energy storage. In contrast to water splitting, where the oxygen evolution reaction has multiple electron steps and consequently high overvoltage losses, iodide and bromide have rapid kinetics for their reactions. Subsequently, a much lower overvoltage is required, leading to correspondingly lower energy losses. If one considers the round-trip efficiency of the electrolysis-fuel cell combination, the rapid kinetics for HI and HBr as compared to water give them a higher round-trip efficiency. Additionally, if the bromine and iodine could be used for chemical processing, then the hydrogen could be used in an oxygen fuel cell, greatly increasing the overall efficiency of the system. The difficulty of dealing with highly corrosive materials such as bromine and iodine is an important matter. That will certainly limit their practical application to any energy storage system.

at \$75/bbl oil ??









Inductive Approaches to Materials Discovery and Optimization

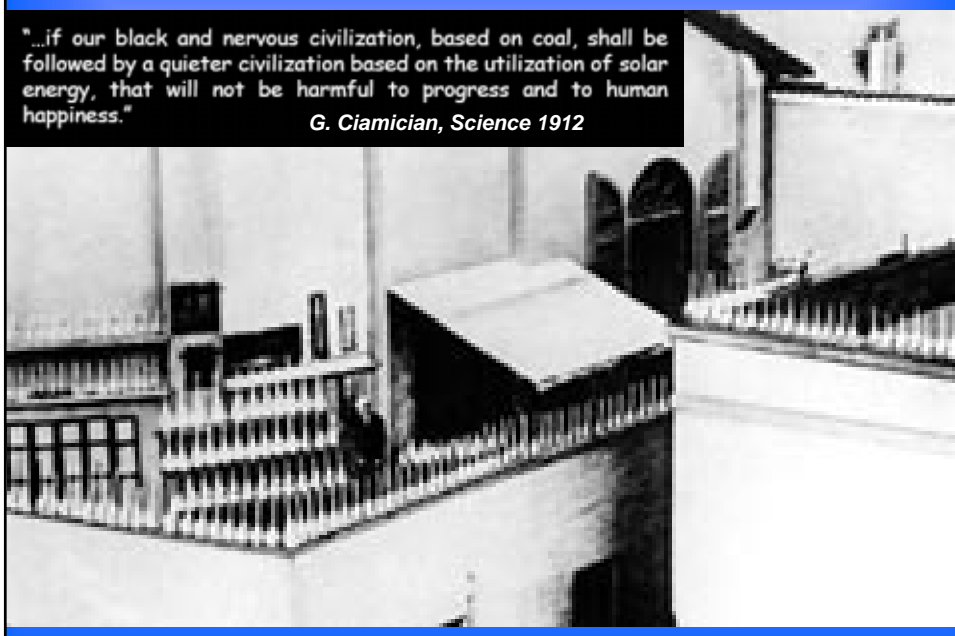


Countless Unseen Details Are Often the Difference Between Mediocre and Magnificent

Giacomo Ciamician, University of Bologna, 1910

"...if our black and nervous civilization, based on coal, shall be followed by a quieter civilization based on the utilization of solar energy, that will not be harmful to progress and to human happiness."

G. Ciamician, Science 1912

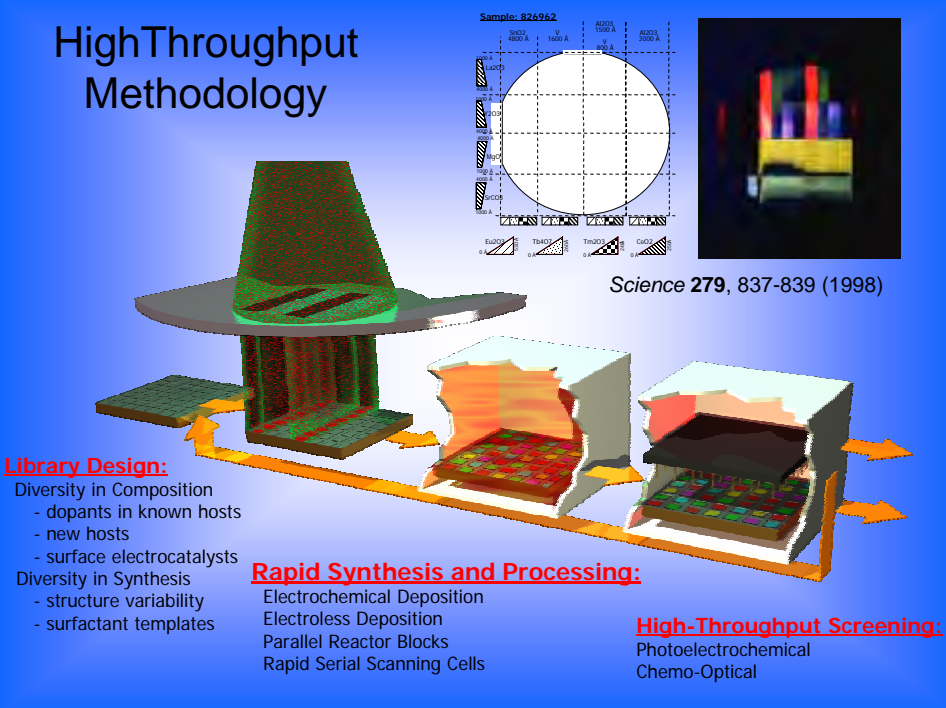


Parallel (“combinatorial”) Experimentation

An Old Methodology NOT a New Field

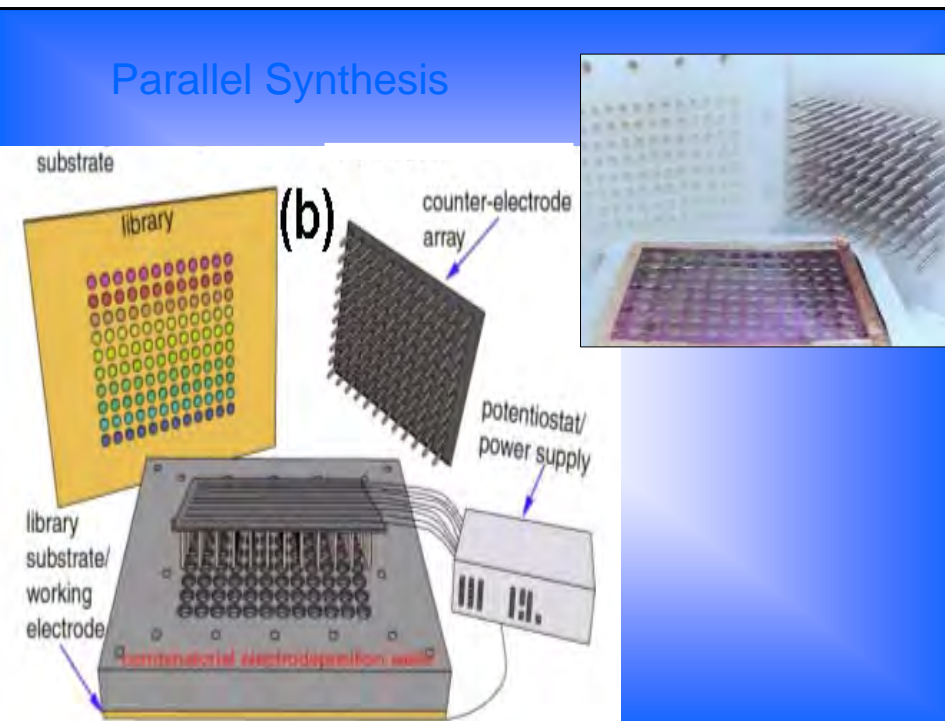
- ~ 400 bce Plato, Socrates - Induction
- ~ 1600 Sir Francis Bacon
- ~ 1840's Thomas Edison (G.E.)
- ~ 1900 Ciamician (photocatalysis)
- ~ 1960's Dupont, IBM, and Sarnoff Labs
- 1969 Joe Hanak Phys. Lett. 30A 201-202
Sawatzky and Kay, IBM Report
- 1995 Xiang et al Science
- 1997 Symyx, 2000 HTE, etc.

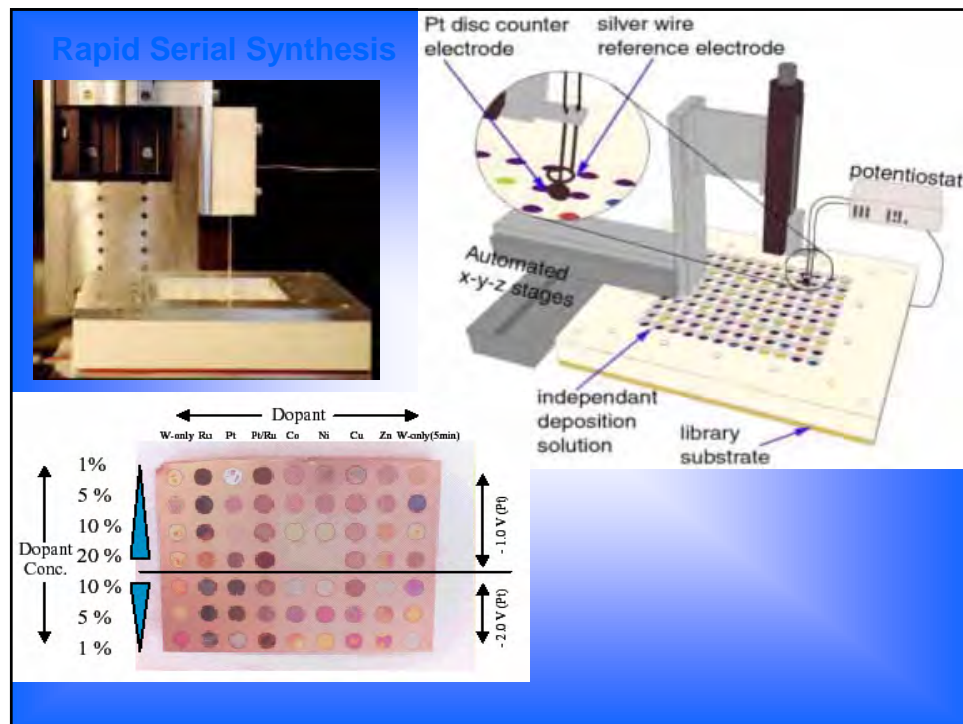
HighThroughput Methodology

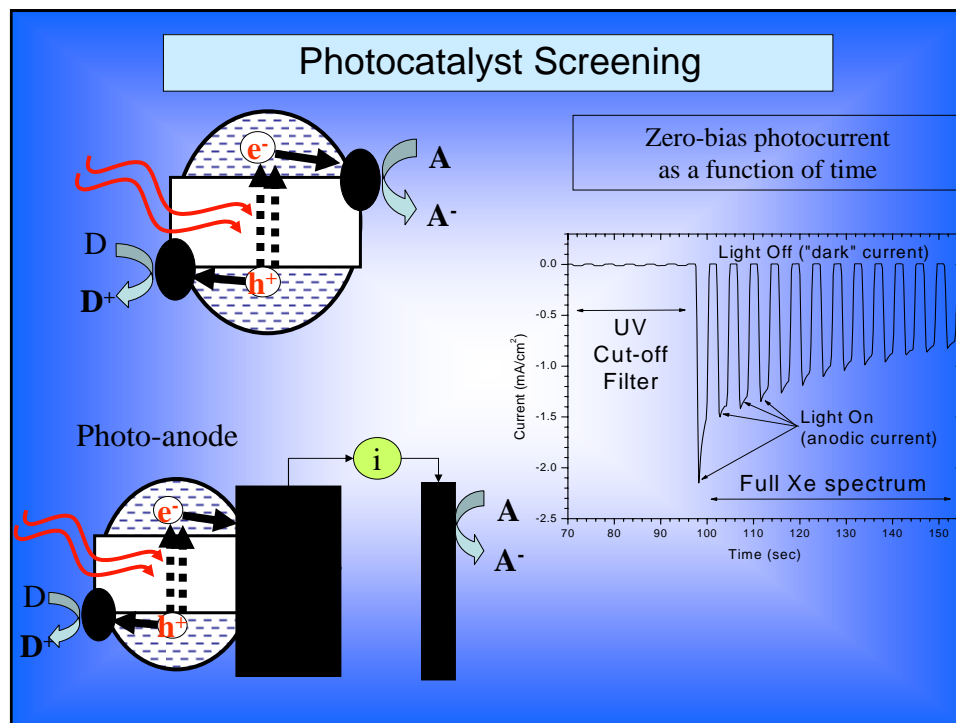
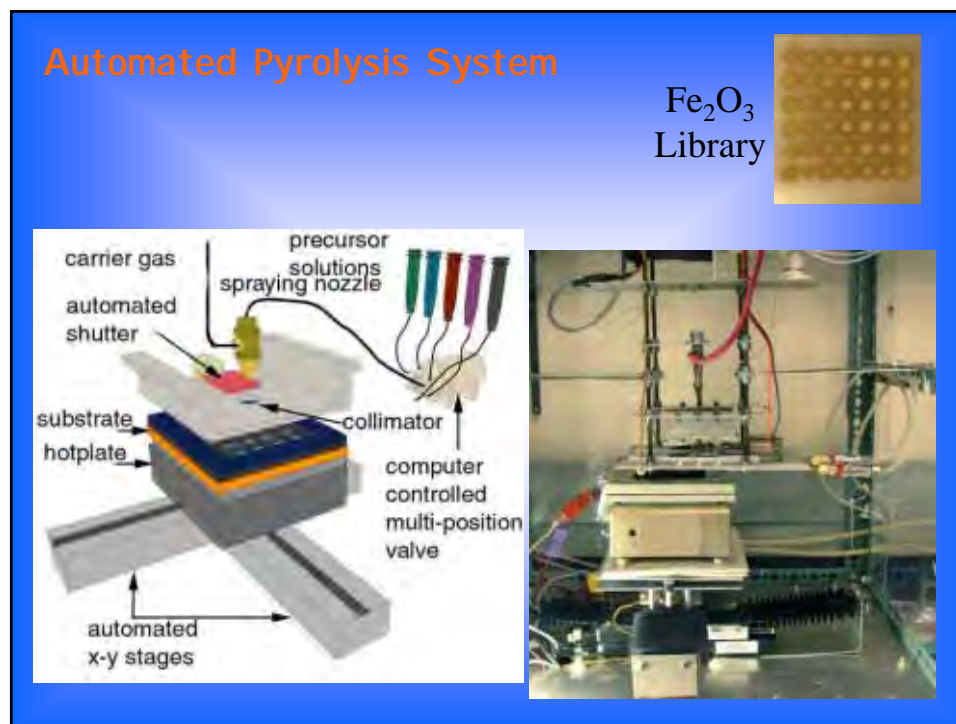


Generalized Electrosynthesis Chemistries

<i>Metal deposition/Oxidation</i>	<i>Metal Oxide Deposition</i>
$M^+ \rightarrow M \rightarrow MO$	Aqueous: $M^+ \rightarrow MOH \rightarrow MO$
1. Metal Electrodeposition $M^{n+} + n e^- \rightarrow M^0$ (Cathodic)	1. MO Deposition electrode: $2 H_2O + 2 e^- \rightarrow H_2 + 2(OH^-)_{sur}$ $[M^{n+}(\text{ligand})] + n(OH^-)_{sur} \rightarrow M(OH)_n$ <u>ligands</u> (acidic) = peroxide (basic) = lactate, citrate, ethylene glycol, acetate
2. Anodization/Anneal $M^0 + H_2O \rightarrow MO + 2 H^+ + 2 e^-$ $M^0 + O_2 \rightarrow MO$	2. Dehydration/Anneal $M(OH)_n \rightarrow MO_{n/2} + \frac{n}{2} H_2O$
Electrochemical Deposition <ul style="list-style-type: none"> • Voltage, Current Density • Electrolyte, Electrode, Dopants • Time, Temperature, pH, Concentration 	Non-Aqueous: $M^+ + O_2 \rightarrow MO$ 1. Direct MO Deposition $xM^{n+} + \frac{y}{2}O_2 + ne^- \rightarrow M_xO_y$ In DMSO etc

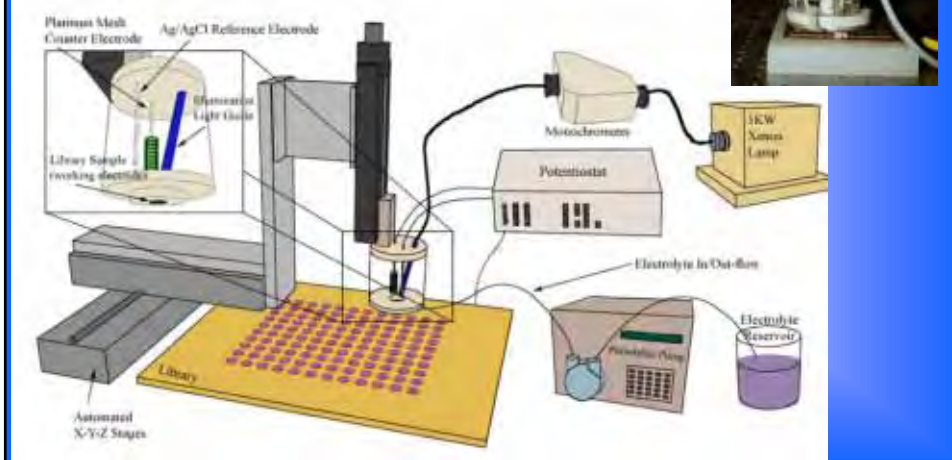




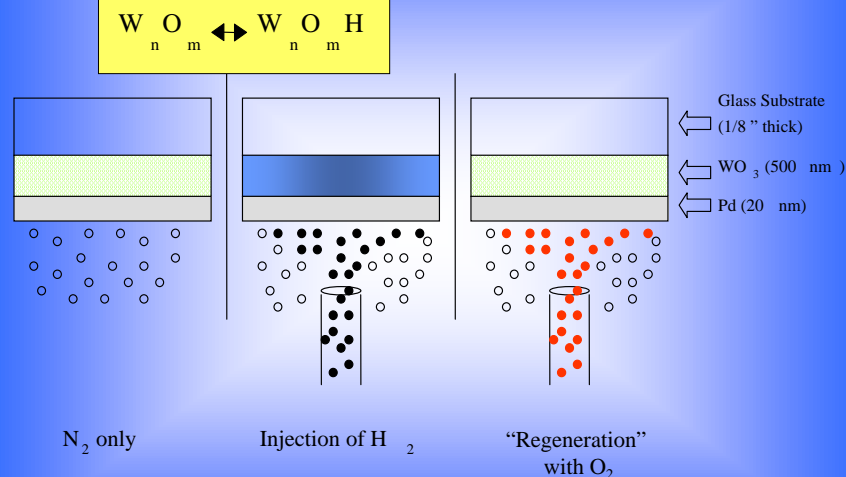


High-Throughput Photoelectrochemical Screening System (HTPESS)

The photoelectrochemical probe (magnified) is symmetrically stepped across the library surface to allow complete photoelectrochemical characterization of each material in the library under computer control.



Chemo-Optical Hydrogen Sensor



Ito, K., and Ohgami, T., *Appl. Phys. Lett.* 60, 8, 938-940 (1992).

Electrocatalytic H₂ Production



J. Combi. Chem. Vol. 4, No. 1 2002

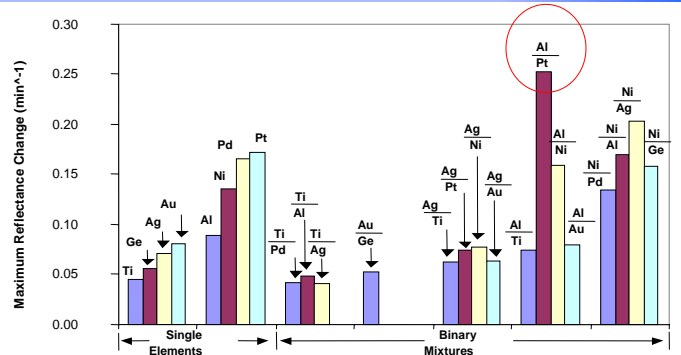
Au	Ge
Ni	Pt
Ag	Al
Ti	Pd
Ti/Pd	Ti/Al
Ti/Ag	Au/Ge
Ni/Pd	Ni/Al
Ni/Ag	Ni/Ge
Ag/Ti	Ag/Pt
Al/Ti	Al/Pt
Al/Ag	Al/Au

All binaries are 80/20 except for Au/Ge which is 50/50.

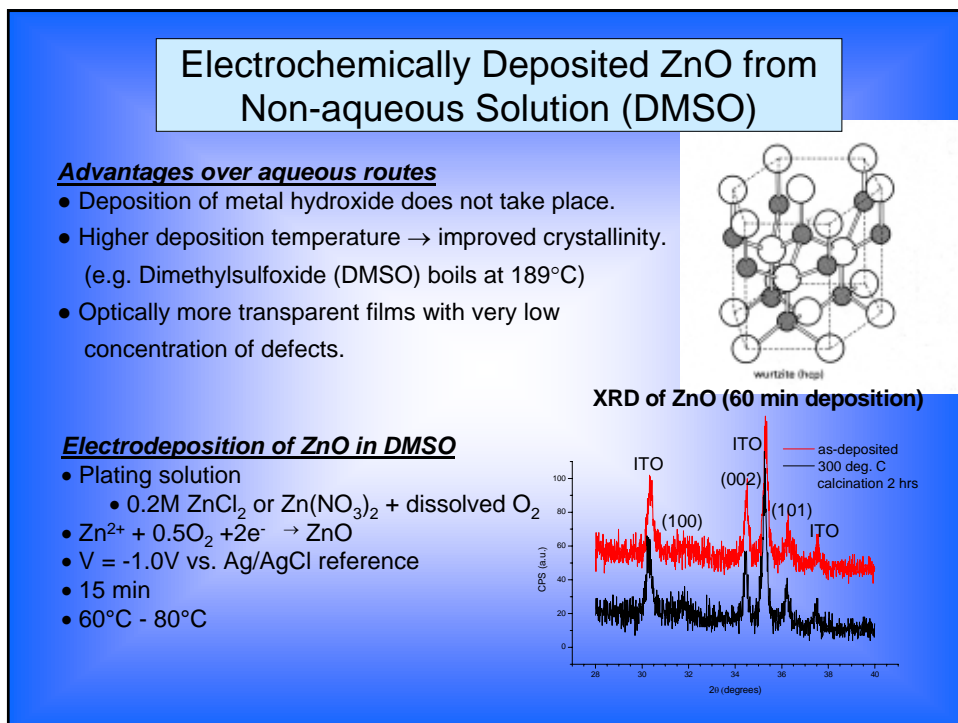
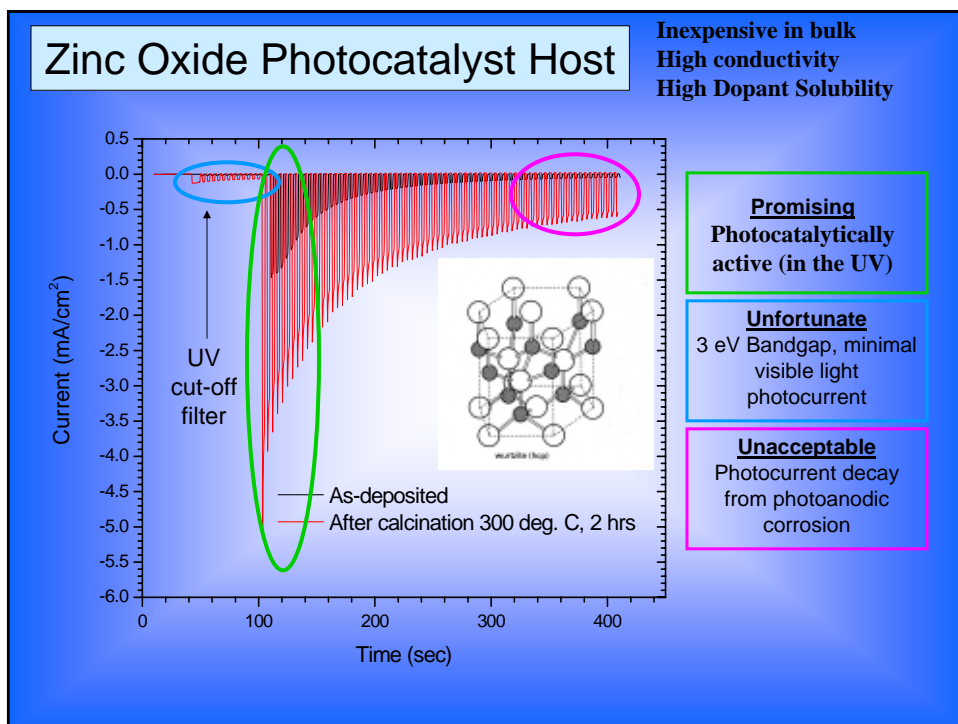
Library of Hydrogen Evolution Electrocatalysts

	A	B	C	D
1	Ti	Pt	Ni	Au
2	Pd	Al	Ag	Ge
3	Ti/Pd	Ti/Al	Ti/Ag	Au/Ge
4	Ni/Pd	Ni/Al	Ni/Ag	Ni/Ge
5	Ag/Ti	Ag/Pt	Ag/Ni	Ag/Au
6	Al/Ti	Al/Pt	Al/Ni	Al/Au

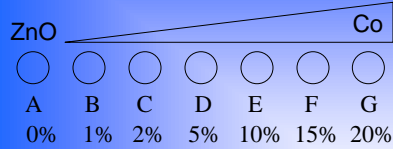
All binaries are 80/20 except for Au/Ge which is 50/50.



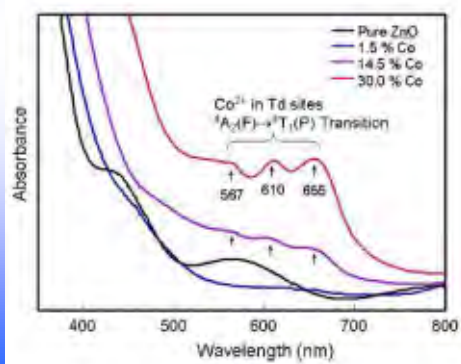
2-D bar graph representing the maximum change in reflectance for each material. Expected trends are validated, as materials containing Ni, Pd, and Pt were the most effective H₂-producers while materials consisting of Ti or Ge performed poorly. The Al/Pt mixture was clearly the best electrocatalyst of those studied.



Problem #1: Improve visible band absorption (doping)



200mM ZnCl₂ in DMSO (saturated O₂)
-1.16V vs. Ag pseudo-reference (-1.0 vs. Ag/AgCl)
85 deg. C 15min deposition onto ITO-coated glass



Ternary ZnO Materials (A_xZn_yO_z)

- 24 different dopants
- 8-12 concentrations (typically 0-20mM or 0-50mM in solution)
- 2-4 replicates
- 500 - 800 ZnO-based films
- Synthesis by
 - “single-sample”
 - “diversity” libraries

Cobalt-doped ZnO showed the most promise for visible absorption. Thus, the next step was to explore this system more deeply.

Dopant	Vis PC	UV PC	Stability in KNO ₃ (aq.)
Ag	Poor	Poor	Average
Al	Good	Average	Good
Au	Poor	Poor	Average
Ce	Average	Average	Excellent
Cd	Poor	Poor	Average
Co	Excellent	Poor	Good
Cr	Poor	Poor	Average
Cu	Poor	Poor	Average
Eu	Poor	Poor	Average
Fe	Good	Good	Average
Mn	Average	Average	Good
Mo	Poor	Poor	Poor
Ni	Excellent	Excellent	Average
Nb	Poor	Average	Good
Pd	Very Poor	Very Poor	N/A
Pt	Poor	Poor	Poor
Rh	Poor	Poor	Aveage
Ru	Excellent	Excellent	Average
Sb	Poor	Poor	Average
Sn	Average	Average	Good
Ti	Very Poor	Very Poor	N/A
V	Poor	Poor	Average
W	precipitated	precipitated	precipitated
Zr	Average	Average	Good

Zn_{1-x}Co_xO Library Design

Solution Co (%)

0.0	0.0	0.0
0.0	1.0	2.0
2.9	4.8	8.3
13.0	17.4	21.3
23.1	25.9	28.6
31.0	33.3	35.5
37.5	39.4	41.2
42.9	44.4	46.0
47.4	50.0	52.9
55.6	57.9	60.0

Film Co (%) by XPS

0.0	0.0	0.0
0.0	0.06	0.1
0.2	0.3	0.5
0.9	1.3	1.6
1.8	2.1	2.4
2.7	2.9	3.2
3.4	3.7	3.9
4.2	4.4	4.6
4.8	5.2	5.6
6.1	6.4	6.8

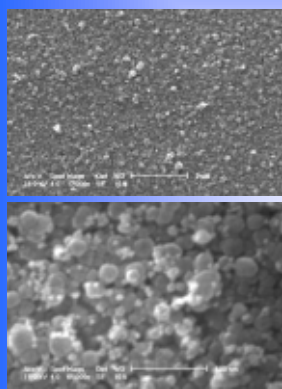
Electrode "priming" row.
To calibrate / equilibrate
electrodes for
temperature and voltage
stability immediately
prior to library synthesis.

Rapid Serial Electrochemical Deposition System (RSEDS)

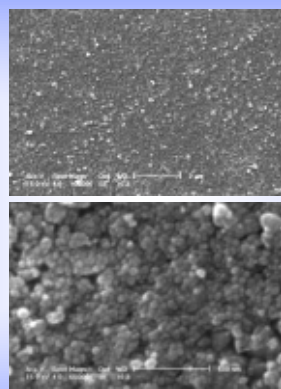
- 120 samples (10x12 array). 27 different Zn:Co ratios with 4 replicates each.
- 100mM ZnCl₂ & 60mM LiNO₃ in DMSO with varying concentrations of Co(NO₃)₂.
- 1.5mL of electrolyte solution. Sample size ~ 8mm diameter.
- Potentiostatic deposition @ -1.15V vs. Ag-wire (-1.0V vs. Ag/AgCl) reference
- Coiled Pt wire counter electrode
- Substrate: Pilkington TEC-15™ Fluorine-doped Tin Oxide (FTO) coated on glass
- 60 second deposition @ 105 °C (Total time for library synthesis: 4 hrs)
- Calcined 500 °C for 8 hrs.

Zn_{1-x}Co_xO: Morphology by SEM

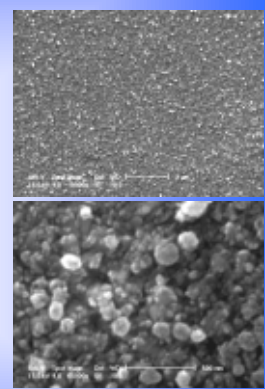
ZnO



Zn_{0.979}Co_{0.021}O

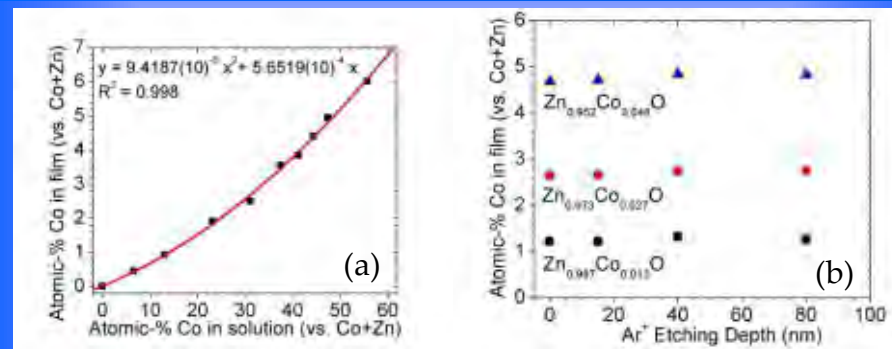


Zn_{0.948}Co_{0.052}O

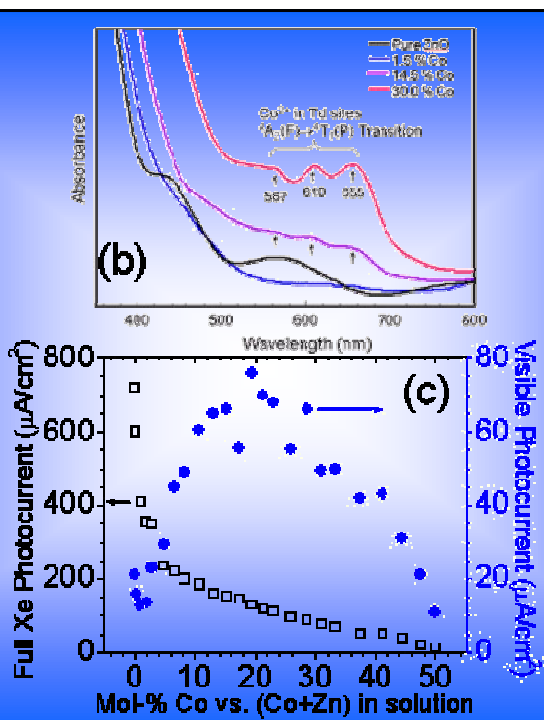


SEM was conducted on 12 selected samples from the library. Film morphology for all samples, regardless of composition, resembled that of pure ZnO. Densely packed particles of 20-200 nm, shaped either as spheres or as platelets, were observed.

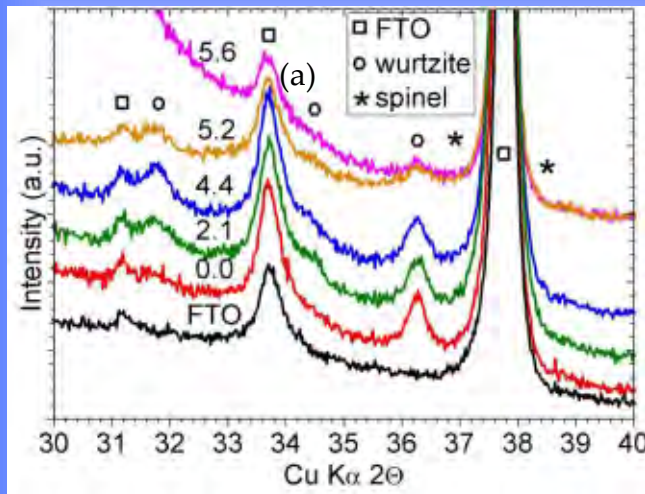
Zn_{1-x}Co_xO: Stoichiometry by XPS



Zn:Co stoichiometry was determined by the ratio of integrated peak areas assigned to Co-2p_{3/2} vs. Zn-2p_{3/2}, after normalizing areas with Scofield sensitivity factors. Graph (a) correlates Zn:Co stoichiometry in the films to Zn:Co ratios in the electrochemical deposition baths. A second-order polynomial was used to fit the data and a relationship was established ($R^2 = 0.998$). The fitted data was used to predict all film compositions within the library (see library design). Graph (b) shows film composition as a function of depth by Ar⁺ etching (4kV, 1.6mA, ~ 5nm/min). Although ion-etching is known to affect surface stoichiometry by selective etching, Zn:Co ratios in the film were found to be fairly consistent at all depths investigated.

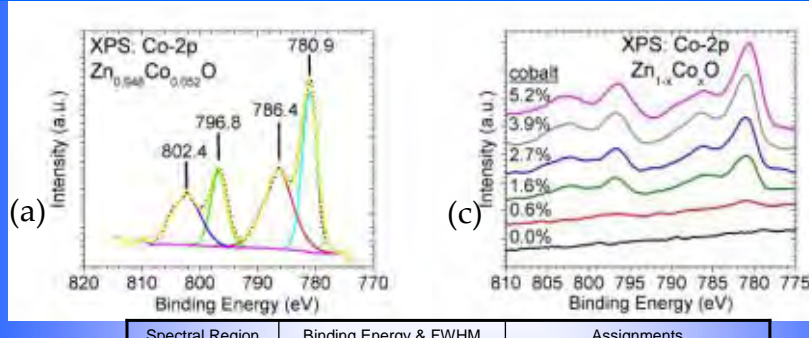


Zn_{1-x}Co_xO: Crystal structure (by XRD)



XRD was performed on selected samples for the purpose of identifying crystal structure of the mixed oxide. All compositions revealed a wurtzite structure typical of pure ZnO. No phase separation of CoO (rocksalt) nor spinel Co₃O₄ was observed, indicating that an atomically mixed Zn_{1-x}Co_xO (wurtzite) was synthesized for all values of x investigated.

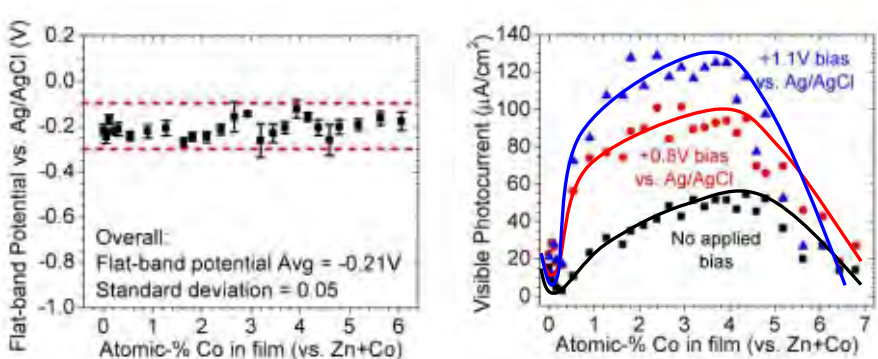
Zn_{1-x}Co_xO: Cobalt oxidation state by XPS



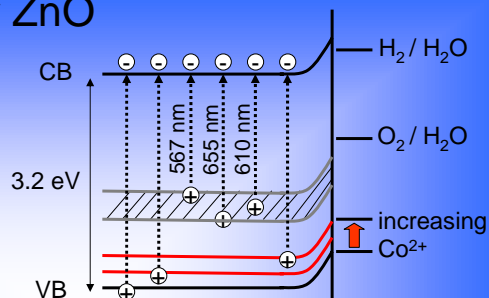
Spectral Region	Binding Energy & FWHM	Assignments
Co-2p _{3/2}	780.9 eV (3.1) 786.4 eV (5.7)	Co ²⁺ multiplet splitting Co ²⁺ shake-up satellite
Co-2p _{1/2}	796.8 eV (3.2) 802.4 eV (5.9)	Co ²⁺ multiplet splitting Co ²⁺ shake-up satellite

XPS was conducted on selected samples to determine Zn:Co stoichiometry as well as the oxidation state of cobalt. Graph (a) reveals the deconvoluted Co-2p spectrum of Zn_{0.948}Co_{0.052}O, in which all four cobalt peaks are assigned to Co²⁺, as indicated in Table (b). Graph (c) compares Co-2p spectra for several different compositions of Zn_{1-x}Co_xO, illustrating that Co²⁺ was the predominant species encountered for all samples.

Zn_{1-x}Co_xO: Flat band potential & Photocurrent under applied bias



Putting it together for ZnO



- Zn:Co film stoichiometries are well-controlled with Co mol-% < 7 %.
- Co(II) is the predominant valency of cobalt
- Only the Wurtzite structure is observed by XRD: No evidence of Rocksalt CoO, Spinel Co₃O₄ or ZnCo₂O₄
- A solid solution is formed, with Co(II) most-likely substituting Zn(II).
- The conduction band edge changes negligibly as a function of composition (for the cobalt range under exploration (< 7%).
- A Co(II) "defect band" emerges within the ZnO bandgap approximately 2 eV below the conduction band.
- The valence band is systematically raised by several tenths of an eV as cobalt concentrations increase.

Compositional Dependencies in Metal Oxide Photocatalysts

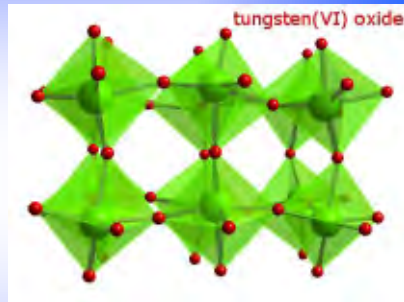
Electrodeposition of WO_3 Based Libraries

➤ WO_3

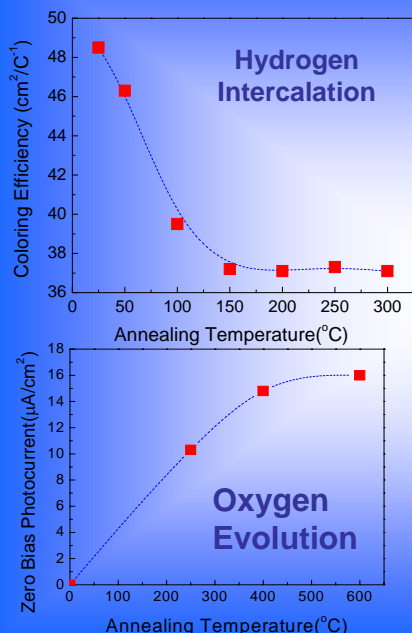
- Stable in electrolytes
- Inexpensive
- Good host for dopants
- Electrochromic ($[\text{Cat}^+]$)

• BUT

- Low CBM
- Previously no ZBPC
- Bandgap ~2.8eV

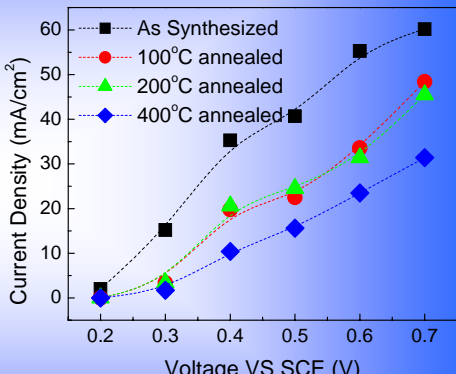


Electrodeposition and Processing of WO_3

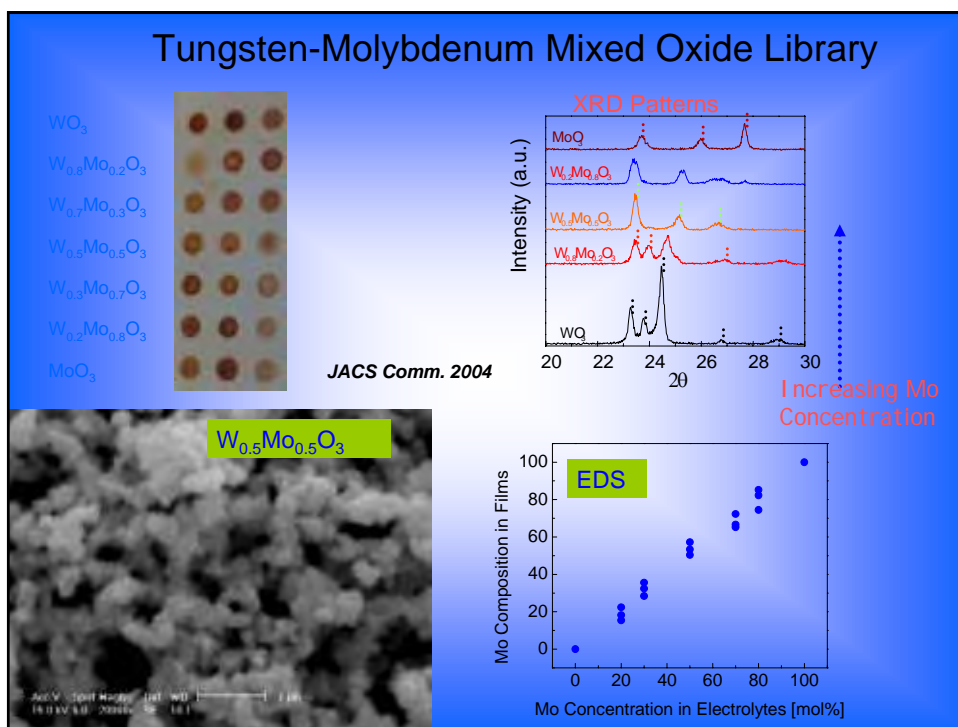
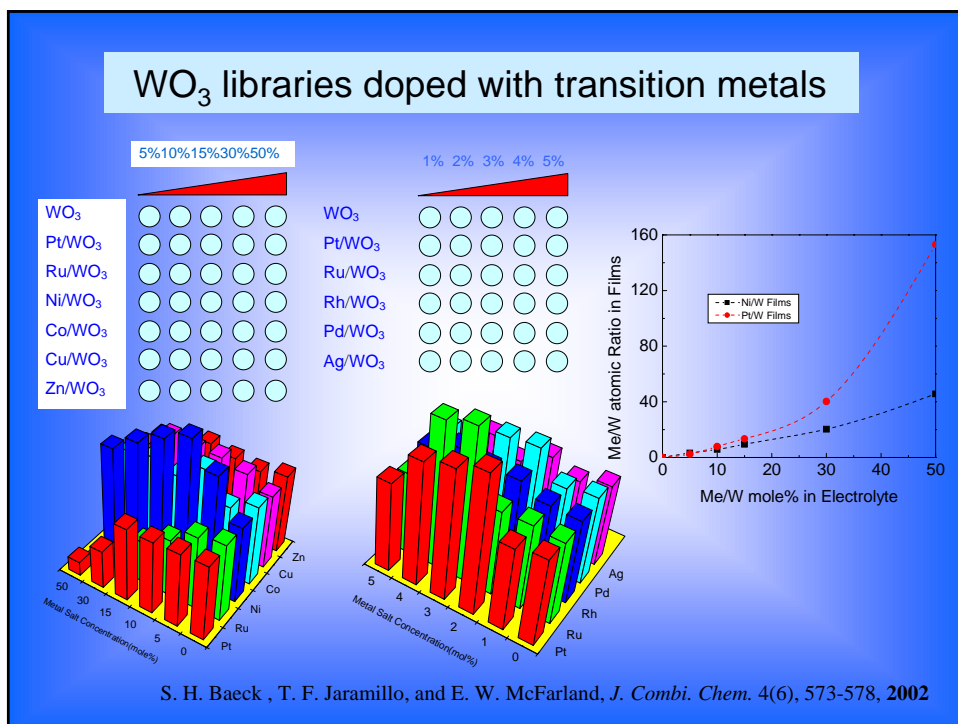


Deposition via peroxide, calcine in air

Methanol Electroxidation

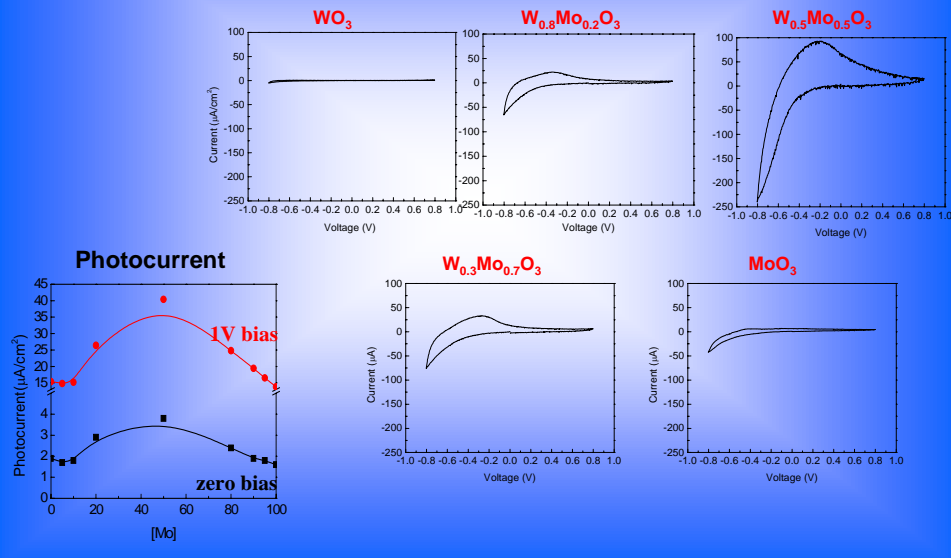


Zero Bias Photocurrent !
Electrodeposition => increased n-type doping
PROCESSING MATTERS !



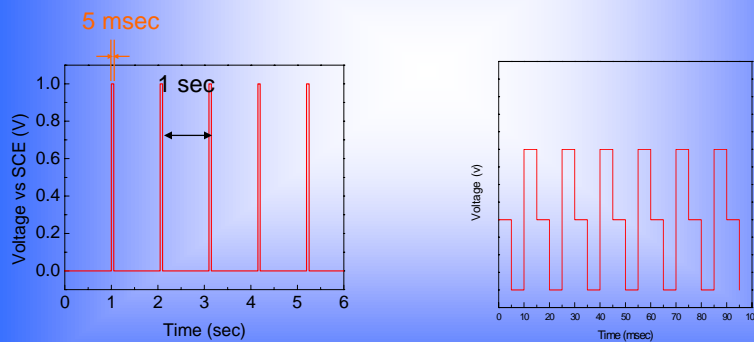
Tungsten-Molybdenum Mixed Oxides

Cyclic Voltammograms in 0.5M KNO₃ for K⁺ Intercalation



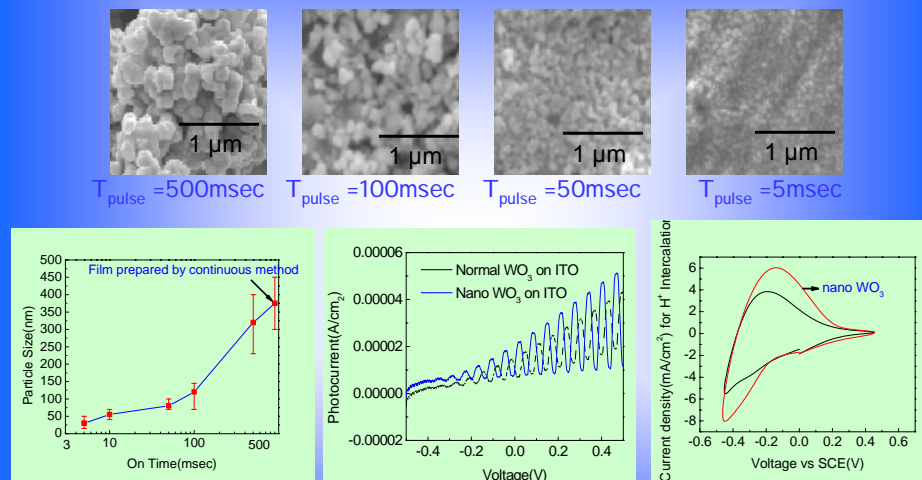
➤ Pulse Electrodeposition

1. Formation of isolated nuclei
2. Growth to larger particles
3. Coalescence of larger particles
4. Formation of a linked network
5. Formation of a continuous deposit



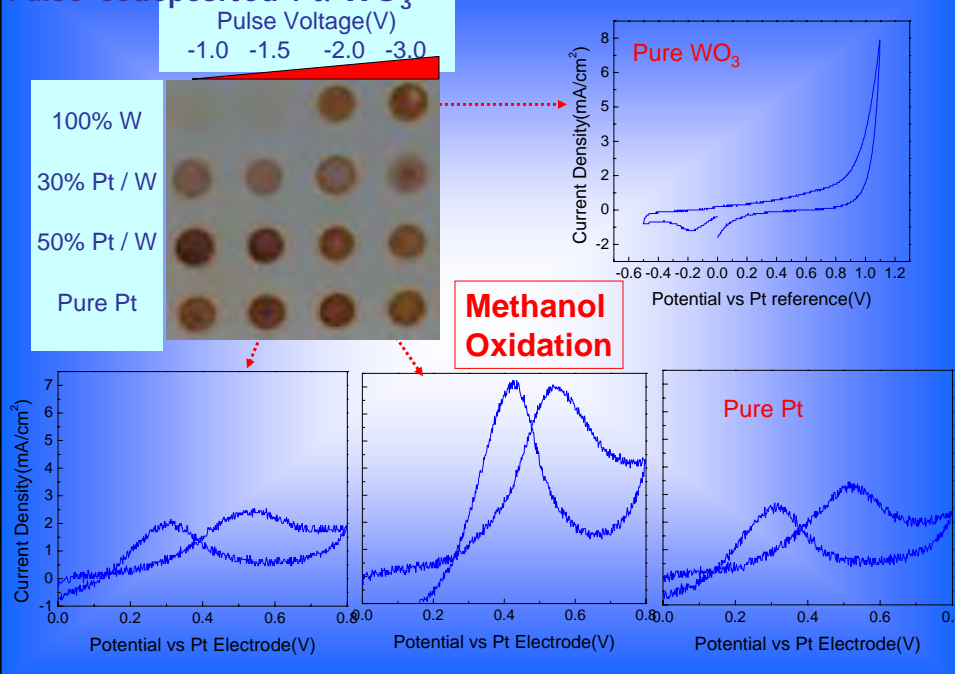
❖ Pulse Parameters : Pulse time, Pulse V, Off time (toff), Total deposition time

Electrodeposition of nanocrystalline WO_3 by pulsed deposition



- S.H.Baeck, T. Jaramillo, G.D.Stucky, and E.W.McFarland, *Nano Letters*, 2(8), 831(2002).

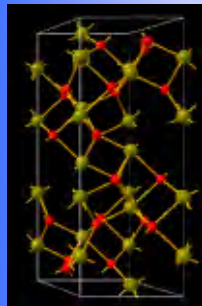
Pulse codeposited Pt/WO₃



Points

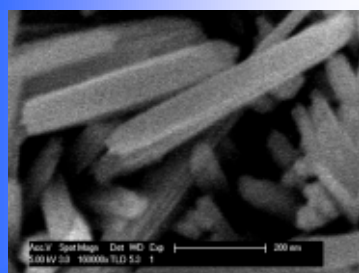
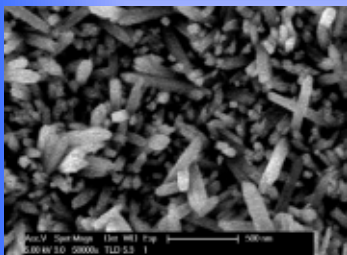
- Successful electrosynthesis of WO_3 , and substituted/doped WO_3 from peroxy complex
 - Electrodeposited Mo substitution preserves unstable monoclinic phase to high concentrations
=> **metastable materials are useful.**
 - ZBPC !
 - Increased cation intercalation
 - No success as yet at decreasing effective gap.

Iron Oxide as a PEC material



R -3 c (167) – trigonal
 $a=5.0380 \text{ \AA}$ $c=13.7720 \text{ \AA}$

Fe_2O_3 Nanorods



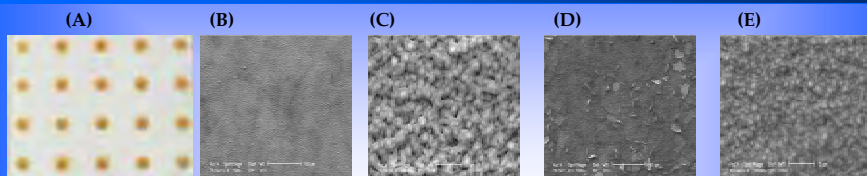
Sample 1- FeCl_3
Sample 2- FeCl_3 -doped Ti
95 °C, 22hr growth

FeCl_3 -Doped Ti was unsuccessful
→ Can we use electrochemistry and self assembly
Methods together??



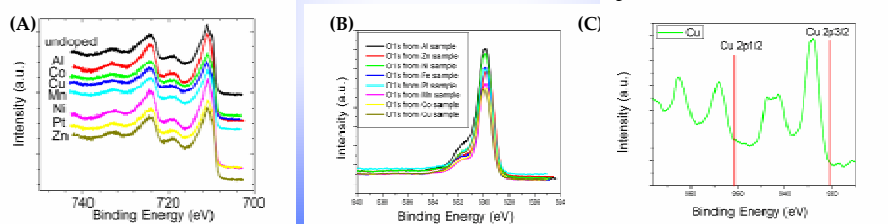
Lionel Vayssières et al. *Chem. Mater.*, Vol. 13, No. 2, 2001

Iron Oxide Deposited by ASPDS



(A) Photograph of a 5x4 library (spacing = 0.125 in.) (B,C) SEM images of a film with 62.5% water (D,E) SEM images of a film with 52.5% water. Changes in morphology are observed as a function of water content in the electrolyte.

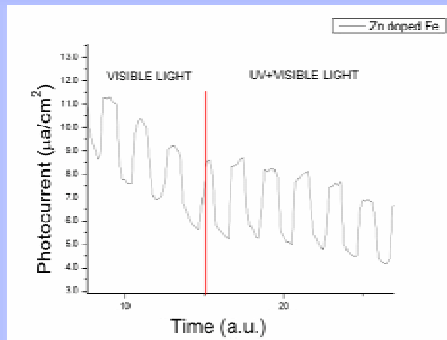
Film Characterization by XPS



XPS data of iron oxide samples deposited by ASPDS (A) XPS data of Fe-2p on different doped iron oxide materials (B) XPS data of O-1s (C) XPS data of Cu-2p on the Cu-doped sample

Photoelectrochemical Screening of Fe₂O₃ materials synthesized by ASPDS

Zero bias photocurrent was measured under UV-vis and vis-only radiation.



Photocurrent from iron oxide doped with Zn (30%) deposited by spray pyrolysis (~ 1 W/cm² illumination)

Preliminary Conclusions: The ASPDS can reliably and reproducibly synthesize samples; several steps are being taken to improve the crystallinity of iron oxides.

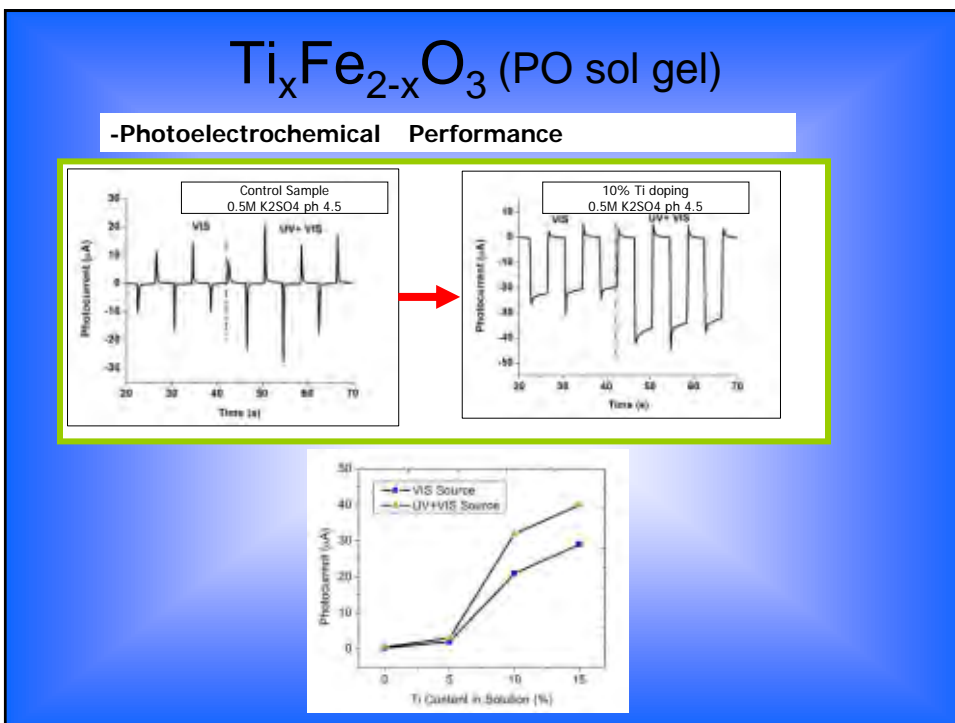
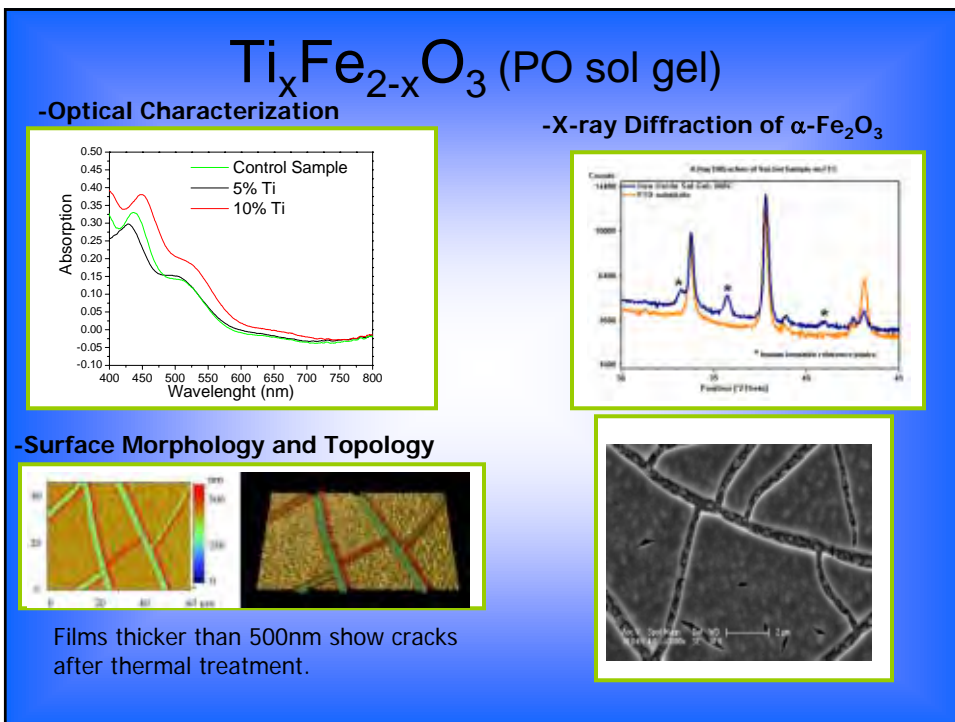
Sol Gel Synthesis

Sol Gel Synthesis

- Single sample technique amenable for combinatorial synthesis
- Complex chemistry
- High degree of control based on kinetics and solvent evaporation
- Thickness limitations (>1 um) on a single processing step
- Soft chemistry method
- Inexpensive compared to other methods
- Requires minimal investment

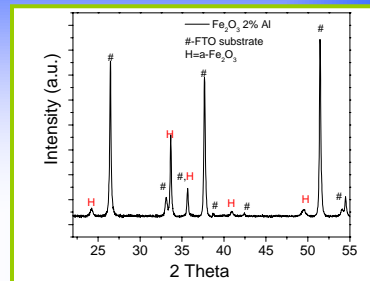
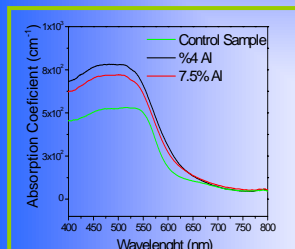


PO-Sol Gel	PVP- Sol Gel
Pros -Amenable for powders -Solubility of most precursors	Pros -High stability of sol gel -Viscosity is determined by the polymer
Cons -Complex gelling due to kinetics -Thickness variation -Limited stability of gel	Cons -Limited solubility of precursors -Use of polymers and metal organics



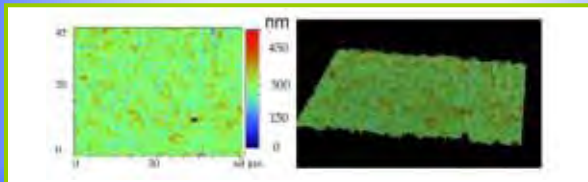
$\text{Al}_x\text{Fe}_{2-x}\text{O}_3$ (PO sol gel)

-Optical Characterization



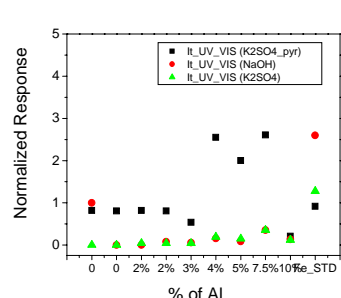
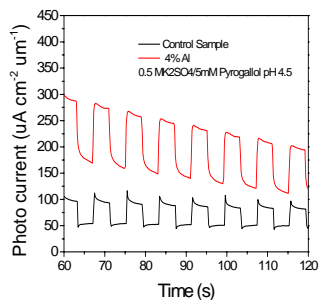
-Surface Morphology and Topology

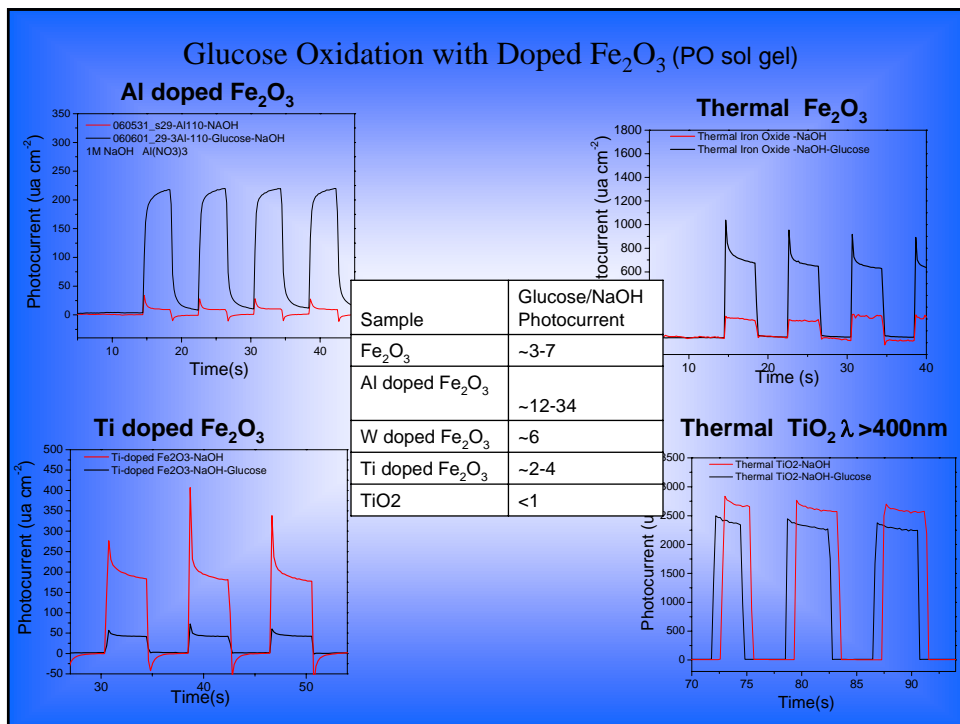
Hematite is the only phase observed



$\text{Al}_x\text{Fe}_{2-x}\text{O}_3$ (PO sol gel)

-Photoelectrochemical Performance





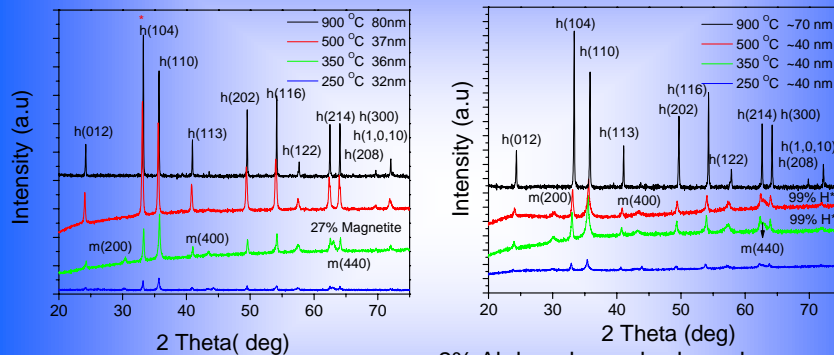
Iron Oxides by PO Sol Gel

Dopant	Type	Type	Improved	Improved	Best
	Expected	Obtained	C.T ¹	P.C ²	Comp.
Ti	N	N	Yes	Yes	X=0.05-0.09
Al	N	N	Yes	Yes	X=0.04-0.075
Ca	P	N-	No	No	
Li	P	N-	No	No	
Cu	P	N-	No	No	
Ni	P	N-	No	No	
Ag	P	N-	No	??	
Mg	P	N-	No	No	

Other dopant materials that will be used: Zn, W, In, V, Cr, Mn

C.T.¹=Charge Transport, P.C.²=Photocurrent

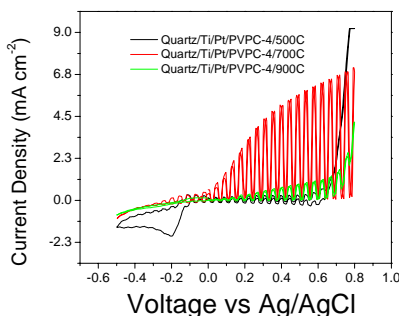
XRD of Hematite Powders



Undoped powder is crystalline at 500°C. Weak magnetic behavior is observed for the powder calcined below 350 °C.

2% Al doped sample shows less crystallinity bellow 900 °C. Due to poor crystallinity the Magnetite phase is also diminished. No Al_2O_3 was present in the XRD.

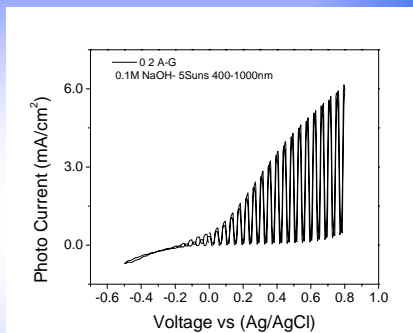
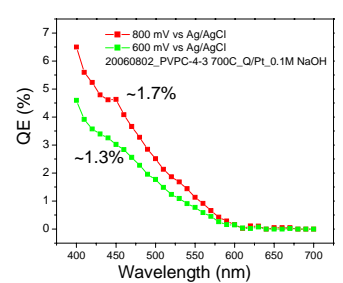
Processing Temperature (poly vinyl pyridine sol gel)



0.5M NaOH 400nm-1000nm 500 mW/cm²

Samples calcined at 700 °C have the best performance, samples calcined at 900 °C show $\text{Fe}_3\text{Ti}_3\text{O}_{10}$, which renders the photoanode inactive.

IPCE of Samples PVP- Fe_2O_3 : NaOH

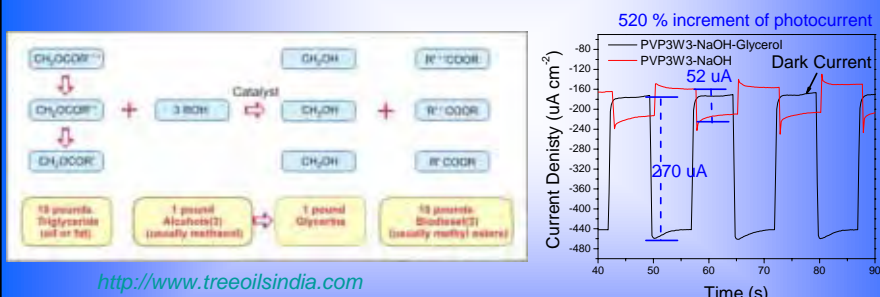


$$QE(\%) = \frac{\# electrons}{\# photons} = \frac{j_p(\lambda)}{e_0 I_0(\lambda)} * 100$$

$$Efficiency(\%) = \frac{j_p(1.23 - E_{app})}{I_0} * 100$$

Hydrogen Production From Glycerol On $\alpha\text{-Fe}_2\text{O}_3$ (PVP sol gel)

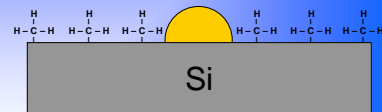
This photo-induced oxidation is not restricted to glucose. The rate of oxidation of fructose, sorbitol and glycine was observed to be much higher under illumination conditions



Silicon ???

1) Methyl terminated Si wafer passivation*

- H-terminated Si
- Cl-terminated via. $\text{PCl}_5 + \text{hv} \rightarrow$ radical chlorination
- Methyl-terminated via. CH_3Li
- Subsequent Pt deposition
 - Electrochemically
 - is limited to defects in CH_3 termination[#]
 - BHF / Pt^{4+} soln.
 - Should also be confined to defects
 - Pt deposition first, followed by methylation



Si

Active NP sites remain exposed

2) Metal oxide Si wafer passivation

- Surface Sol-gel Process (SSP)^{**}
 - Deposition of virtually any metal oxide with monolayer control
 - Requires OH – terminated surface
 - Selective deposition on Si vs. NP surface OH-termination
 - Purely inorganic passivation layer for long term stability
 - Electrical passivation



- Either method works well with planar electrodes and is easily amenable to powders

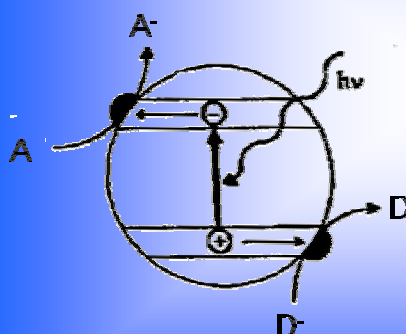
* Lewis, N., Weinberg, H., et. al.

[#] Nakato, Y., et. al. J. Electrochem. Soc., 153 (2) E38-E43 (2006)

^{**}Chem. Mater. 1997, 9, 1296-1298

Summary

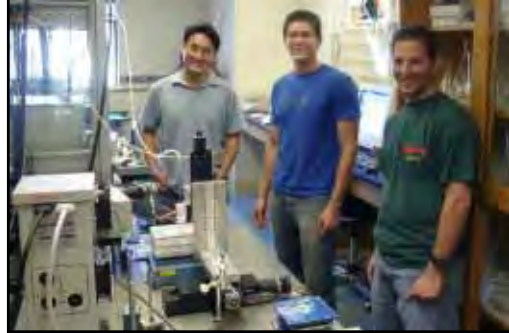
- Development of new photoelectrocatalytic materials is a multifactorial chemical, materials and engineering problem.
- Economics will determine the eventual success of PEC in the energy sector.
- As yet, no suitable materials or forms have been identified.



Acknowledgements

S.H.-Baeck, T.F. Jaramillo,
A.Kleiman, A. Forman,
W. Tang, G. Stucky

\$\$ Funding \$\$
UCSB
College of Engineering
DOE



Questions ?